

RESEARCH ARTICLE

Crosstalk between androgen receptor and WNT/ β -catenin signaling causes sex-specific adrenocortical hyperplasia in mice

Rodanthi Lyraki¹, Anaëlle Grabek¹, Amélie Tison¹, Lahiru Chamara Weerasinghe Arachchige¹, Mirko Peitzsch², Nicole Bechmann^{2,3}, Sameh A. Youssef^{4,5}, Alain de Bruin^{4,6}, Elvira R. M. Bakker⁷, Frank Claessens⁸, Marie-Christine Chaboissier¹ and Andreas Schedl^{1,*}

ABSTRACT

Female bias is highly prevalent in conditions such as adrenal cortex hyperplasia and neoplasia, but the reasons behind this phenomenon are poorly understood. In this study, we show that overexpression of the secreted WNT agonist R-spondin 1 (RSPO1) leads to ectopic activation of WNT/ β -catenin signaling and causes sex-specific adrenocortical hyperplasia in mice. Although female adrenals show ectopic proliferation, male adrenals display excessive immune system activation and cortical thinning. Using a combination of genetic manipulations and hormonal treatment, we show that gonadal androgens suppress ectopic proliferation in the adrenal cortex and determine the selective regulation of the WNT-related genes *Axin2* and *Wnt4*. Notably, genetic removal of androgen receptor (AR) from adrenocortical cells restores the mitogenic effect of WNT/ β -catenin signaling. This is the first demonstration that AR activity in the adrenal cortex determines susceptibility to canonical WNT signaling-induced hyperplasia.

KEY WORDS: R-spondin signaling, Androgen receptor, Adrenocortical hyperplasia, Sexual dimorphism

INTRODUCTION

Sexual dimorphism is prevalent among mammalian phenotypic traits (Karp et al., 2017) and underlies several aspects of mammalian physiology, including malignant transformation (Clocchiatti et al., 2016) and immunity (Klein and Flanagan, 2016). Sex-specific effects often stem from the action of gonadal hormones (Yu et al., 2020) but can also have sex chromosome-related causes, such as the

incomplete inactivation of X chromosome genes (Chen et al., 2012). An important open question is whether sex impacts size maintenance and homeostasis of self-renewing adult tissues, such as the adrenal cortex.


Adrenals are endocrine organs consisting of a non-endocrine capsule surrounding the outer cortex, responsible for the synthesis of steroid hormones, and the inner medulla, responsible for the synthesis of catecholamines. The adrenal cortex is characterized by the expression of the transcription factor SF1 (*Nr5a1*) and is further divided into concentric rings that form a characteristic zonation pattern (Pignatti et al., 2017). The outer zona glomerulosa (zG) produces mineralocorticoids, the middle zona fasciculata (zF) produces glucocorticoids, and the inner zona reticularis (zR) produces androgens. The latter is absent in mice; in its place, we find the X-zone, a transient remnant of the fetal adrenal with unknown functions in adulthood (Huang and Kang, 2019).

The adrenal cortex undergoes constant renewal owing to resident populations of stem/progenitor cells that are primarily concentrated in the capsule and the sub-capsular zG (Ching and Vilain, 2009; Finco et al., 2018; King et al., 2009; Lyraki and Schedl, 2021b). A proliferating zone can be distinguished in the outer cortex that gradually fades out towards the inner part; as a result, the inner zF is largely composed of quiescent cells (Chang et al., 2013). Proliferation arrest coincides with transdifferentiation of zG cells to a zF identity and centripetal migration (Freedman et al., 2013).

Canonical WNT/ β -catenin signaling has a prominent position among the molecular pathways that participate in maintaining adrenal cortex homeostasis and zonation (Kim et al., 2008; Leng et al., 2020). Dramatic interventions such as the constitutive activation of β -catenin lead to the expansion of the zG at the expense of the zF and tumor development in aging mice (Berthon et al., 2010; Pignatti et al., 2020). Other mechanisms allow for a more precise fine-tuning of WNT activation levels in the adrenal cortex, such as the negative feedback loop that attenuates WNT signaling based on the activity of the membrane-bound E3 ubiquitin ligase ZNRF3 (Hao et al., 2012). Secreted ligands of the R-spondin (RSPO) family and their cognate receptors LGR4/5/6 form a complex that can bind and remove ZNRF3 from the cell surface, thus potentiating WNT signaling (Nusse and Clevers, 2017; Zebisch et al., 2013). In the mouse adrenal cortex, a diminishing gradient of WNT signaling activity from the zG to the zF is maintained via the localized expression of secreted WNT potentiators, mainly *Wnt4* in the zG, and R-spondins (*Rspo1* and *Rspo3*) in the capsule, and ensures a normal organ size (Basham et al., 2019; Heikkilä et al., 2002; Vidal et al., 2016). Although this knowledge originates mostly from mouse genetic studies, the high prevalence of *CTNNB1* and *ZNRF3* driver mutations in human adrenocortical carcinoma (ACC) shows the relevance of these pathways for human adrenal disease (Assié et al., 2014; Zheng et al., 2016).

¹Université Côte d'Azur, Inserm, CNRS, Institut de Biologie Valrose, 06108 Nice, France. ²Institute of Clinical Chemistry and Laboratory Medicine, University Hospital Carl Gustav Carus, Technische Universität Dresden, Fetscherstrasse 74, 01307 Dresden, Germany. ³Department of Medicine III, University Hospital Carl Gustav Carus, Technische Universität Dresden, Fetscherstrasse 74, 01307 Dresden, Germany. ⁴Dutch Molecular Pathology Center, Department of Biomolecular Health Sciences, Faculty of Veterinary Medicine, Utrecht University, 3584 CL, Utrecht, the Netherlands. ⁵Janssen Research and Development, 2340 Beerse, Belgium. ⁶Department of Pediatrics, University of Groningen, University Medical Center Groningen, 9713 AV, Groningen, the Netherlands. ⁷Department of Pathology, University Medical Center Utrecht, 3508 AB, Utrecht, the Netherlands. ⁸Molecular Endocrinology Laboratory, Department of Cellular and Molecular Medicine, KU Leuven, 3000 Leuven, Belgium.

*Author for correspondence (schedl@unice.fr)

 R.L., 0000-0003-4974-5567; L.C.W., 0000-0003-4492-8946; M.P., 0000-0002-2472-675X; N.B., 0000-0002-6932-333X; A.d.B., 0000-0001-8579-2649; A.S., 0000-0001-9380-7396

This is an Open Access article distributed under the terms of the Creative Commons Attribution License (<https://creativecommons.org/licenses/by/4.0>), which permits unrestricted use, distribution and reproduction in any medium provided that the original work is properly attributed.

Handling Editor: Monica J. Justice
Received 20 December 2022; Accepted 29 March 2023

The adrenal gland is recognized as one of the most sexually dimorphic non-reproductive organs. For example, many forms of adrenocortical hyperplasia and neoplasia associated with endocrine manifestations, such as Cushing's syndrome, are more frequent among women than men (Lyraki and Schedl, 2021a). This includes benign adrenocortical adenomas (female:male ratio, 4-8:1) (Lacroix et al., 2015; Lindholm et al., 2001) and ACCs (female:male ratio, 1.5-2.5:1) (Ayala-Ramirez et al., 2013; Luton et al., 1990; Scollo et al., 2016). Under normal homeostatic conditions, the mouse adrenal shows a strong dimorphism (Bielohuby et al., 2007; Grabek et al., 2019) and we recently showed that adrenocortical renewal is more rapid in female than in male mice, due to higher activity of cortical AXIN2⁺ progenitors and female-specific recruitment of capsular GLI1⁺ progenitors (Grabek et al., 2019). Sex hormones are implicated in these processes and modulate signaling pathways via yet unknown mechanisms (Dumontet et al., 2018; Grabek et al., 2019).

Even though testicular androgens influence the adrenal cortex, whether this influence is direct and how this influence translates to a reduced susceptibility to hyperplasia is still obscure. To answer these questions, we used a mouse model of disrupted adrenal homeostasis owing to the ectopic expression of *Rspo1* in the adrenal cortex, thus causing moderate WNT signaling hyperactivation. This genetic manipulation results in ectopic proliferation and hyperplasia in female mice, in contrast to cortical thinning and degeneration in males. We show that sexual dimorphism in our model is dependent on testicular androgens, which act directly on adrenocortical cells through their cognate receptor AR (androgen receptor) to cause cell cycle arrest and counteract the mitogenic effect of enhanced WNT signaling.

RESULTS

Ectopic expression of *Rspo1* leads to sex-specific adrenocortical hyperplasia or degeneration

In order to generate a mouse model for adrenocortical hyperplasia, we sought to disrupt the gradient of canonical WNT signaling activation by ectopically expressing R-spondin 1 (RSPO1) in the adrenal cortex. We used a Cre-inducible *Rspo1* gain-of-function (GOF) allele (De Cian et al., 2017; Rocha et al., 2015) and the *Sfl-Cre* transgene that drives Cre recombinase expression in SF1⁺ tissues including the adrenal cortex (Bingham et al., 2006) (*Sfl-Rspo1*^{GOF} mice) (Fig. 1A). In control adult animals, *Rspo1* expression was restricted to the outer adrenal capsule, in agreement with previous research (Vidal et al., 2016). By contrast, *Sfl-Rspo1*^{GOF} mice showed expression throughout the adrenal cortex (Fig. 1B) and dramatically increased total mRNA levels regardless of sex (Fig. S1A).

Ectopic *Rspo1* expression in our models resulted in striking hyperplasia of the adrenal glands in 6-week-old mice (Fig. 1C). Because the *Sfl-Cre* line drives expression of the GOF allele already during embryogenesis, hyperplasia was noticeable in pre-pubertal pups and was comparable between male and female mice at 3 weeks of age (Fig. 1D). After puberty, however, the phenotype evolved in a highly sexually dimorphic manner. Whereas female adrenals from *Sfl-Rspo1*^{GOF} mice further increased in size, male adrenals remained smaller, and their size even regressed as they aged (Fig. 1D; 6 weeks, 6 months and 12 months). Ordinary two-way ANOVA confirmed the interactive effect of sex and *Rspo1* overexpression on adrenal weight at 6 weeks and 6 months ($P < 0.0001$) but not at 3 weeks ($P = 0.46$). Thus, puberty appears to be a critical period for the development of sexual dimorphism in our model.

Next, we conducted a histological analysis to examine the cellular composition of *Sfl-Rspo1*^{GOF} adrenals. According to Hematoxylin and Eosin (H&E) analysis at 6 weeks of age, all the female GOF adrenals analyzed exhibited diffuse atypical hyperplasia in the cortex ($n = 5$) (Fig. 1E). The inner cortex was composed of steroidogenic cells expressing 3 β HSD (encoded by *Hsd3b*), although its expression seemed reduced compared to control adrenals, whereas the medulla was fragmented (Fig. 1F). Male GOF adrenals, however, displayed non-neoplastic degenerative changes in the form of markedly vacuolated, polynucleated cells. At 6 weeks, all the male *Sfl-Rspo1*^{GOF} adrenals ($n = 6$) exhibited these degenerative changes to a varying degree (Fig. 1E), which were negative for the steroidogenic marker 3 β HSD (Fig. 1F). By 3 months of age, degenerative areas expanded significantly in all the male *Sfl-Rspo1*^{GOF} adrenals ($n = 3$), leading to cortical thinning (Fig. S1B). These degenerative changes affected female adrenals to a much lesser degree (2/3 adrenals examined at 3 months displayed only a few abnormal cells) (Fig. S1B). zG expansion is a known consequence of the constitutive activation of β -catenin in the adrenal cortex (Berthon et al., 2010; Pignatti et al., 2020). However, in *Sfl-Rspo1*^{GOF} adrenals, the zG was not expanded in either sex, as shown by immunostaining with the zG markers DAB2 and LEF1 (Fig. S1C,D).

To assess whether ectopic expression of *Rspo1* affected the endocrine activity of the hyperplastic adrenals, we measured plasma steroids of control and GOF animals at 6 weeks of age by liquid chromatography coupled with tandem mass spectrometry (LC-MS/MS). Levels of the mineralocorticoid hormone aldosterone and its precursor 18-OH-corticosterone were not significantly changed among our experimental groups. Levels of the glucocorticoid corticosterone and another steroid hormone precursor, 11-deoxycorticosterone, showed a mild decrease in female and increase in male *Sfl-Rspo1*^{GOF} mice, although none of these changes reached statistical significance (Fig. S2). Analysis of the adrenocorticotrophic hormone-responsive differentiation marker AKR1B7 (Sahut-Barnola et al., 2000) showed loss of expression in subpopulations of cells of the inner cortex, which explains the absence of hormone overproduction despite the striking hyperplasia (Fig. S1E). Plasma levels of the androgens testosterone and dihydrotestosterone (DHT) did not differ significantly among control and *Sfl-Rspo1*^{GOF} mice (Fig. S2).

As the *Sfl-Rspo1*^{GOF} animals aged, the diffuse hyperplasia and cortical thinning gave way to increased frequency of well-circumscribed benign nodules and adenomas (Fig. S3) (6/8 *Sfl-Rspo1*^{GOF} males and 6/8 *Sfl-Rspo1*^{GOF} females of 12 months). Importantly, 1/8 aging *Sfl-Rspo1*^{GOF} females had a well-differentiated adrenal carcinoma with capsular invasion (Fig. S3). None of the controls or male *Sfl-Rspo1*^{GOF} animals displayed any malignant tumor; thus, sexual dimorphism might also characterize tumor progression, but analysis of more animals is required to draw this conclusion.

Taken together, ectopic *Rspo1* expression exerts a highly sexually dimorphic effect on the adrenal cortex. In female mice, it leads to diffuse hyperplasia of the adrenal cortex without increased endocrine activity. On the contrary, male GOF adrenals display expansive degenerative lesions and cortical thinning, although compensating activity of the remaining cortex ensures that insufficiency of steroid hormones is avoided.

Ectopic expression of *Rspo1* leads to female-specific ectopic proliferation

The striking sexual dimorphism in our *Sfl-Rspo1*^{GOF} model is reminiscent of the female bias observed in human adrenal diseases. To further investigate its molecular underpinnings, we conducted

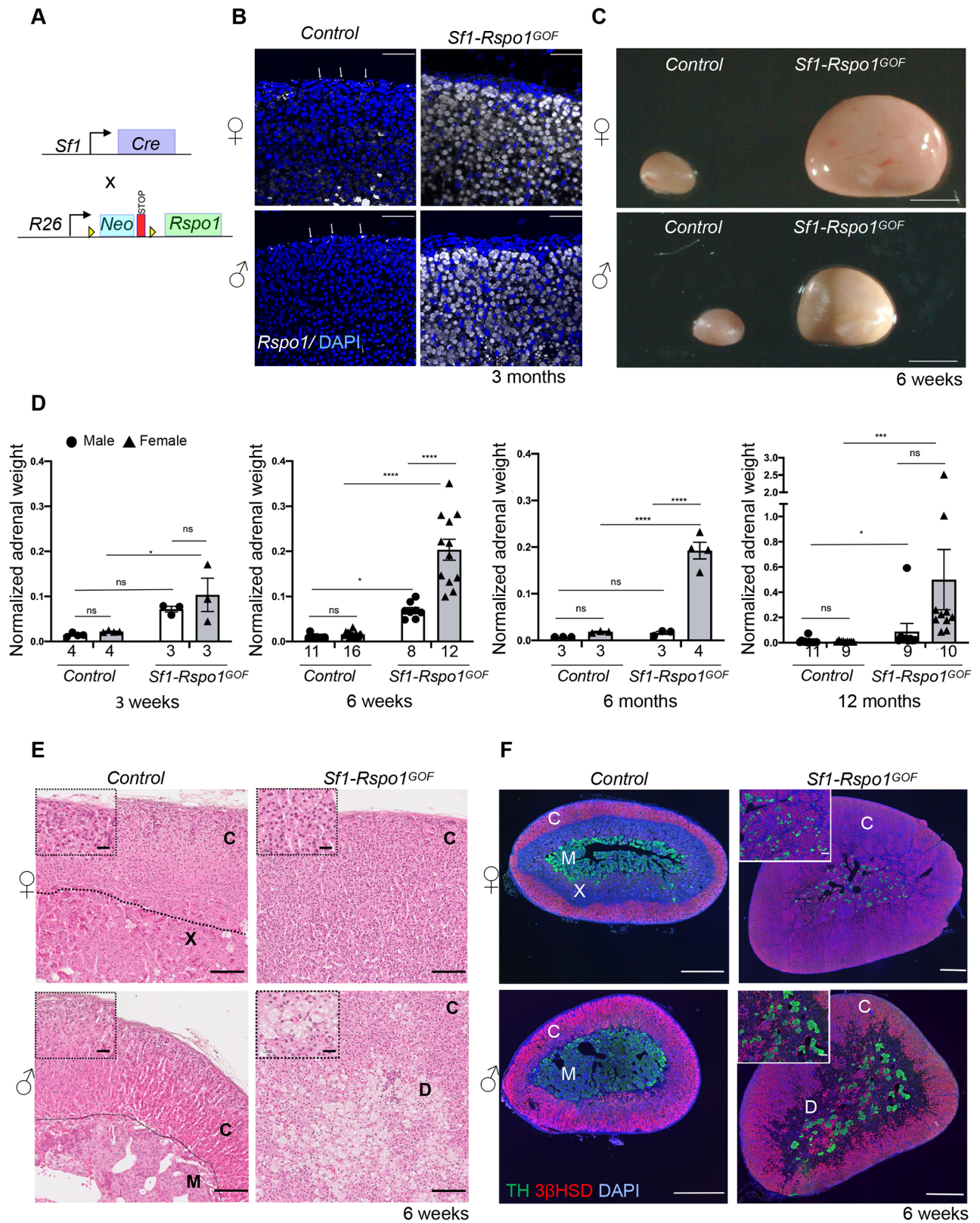


Fig. 1. See next page for legend.

mRNA sequencing and differential expression analysis of whole adrenals from control and *Sf1-Rspo1*^{GOF} mice of both sexes during puberty (at 4 weeks), a timepoint before the occurrence of male-specific degeneration of adrenals (Fig. S4A) [data available

at NCBI's Gene Expression Omnibus (Barrett et al., 2013) with the accession number GSE178958]. As expected, principal component analysis (PCA) identified the presence of the *Rspo1*^{GOF} allele as a major component in our RNA sequencing (RNA-seq) experiment.

Fig. 1. RSPO1 overexpression leads to sex-specific adrenocortical hyperplasia or degeneration. (A) Schematic representation of the genetic strategy to overexpress RSPO1 in steroidogenic cells using *Sfl1-Cre*. (B) *In situ* hybridization for *Rspo1* using RNA Scope technology on adrenal sections from 3-month-old mice. White arrows mark *Rspo1* mRNA molecules. Scale bars: 50 μ m. (C) Representative photographs of adrenal glands from control and *Sfl1-Rspo1^{GOF}* mice at the end of puberty (6 weeks of age). Scale bars: 1 mm. (D) Graphs of mean adrenal weight normalized to body weight at different ages comparing control mice to *Sfl1-Rspo1^{GOF}* mice when ectopic RSPO1 expression is driven by *Sfl1-Cre* (error bars represent s.e.m.). The numbers below the graph columns represent number of samples in each group (*n*). Statistical analysis for 3 weeks, 6 weeks and 6 months was performed using ordinary two-way ANOVA followed by Tukey's multiple comparisons test. Statistical analysis for 12 months was done using a non-parametric test (Kruskal–Wallis test) owing to the non-Gaussian distribution of the data. Adjusted *P*-values for comparisons at 3 weeks: control females (F) versus *Sfl1-Rspo1^{GOF}* F, *P*=0.0192; control males (M) versus *Sfl1-Rspo1^{GOF}* M, *P*=0.1067; *Sfl1-Rspo1^{GOF}* F versus *Sfl1-Rspo1^{GOF}* M, *P*=0.5631. Adjusted *P*-values for comparisons at 6 weeks: control F versus *Sfl1-Rspo1^{GOF}* F, *P*<0.0001; control F versus control M, *P*=0.0239; *Sfl1-Rspo1^{GOF}* F versus *Sfl1-Rspo1^{GOF}* M, *P*<0.0001; control M versus *Sfl1-Rspo1^{GOF}* M, *P*=0.0184. Adjusted *P*-values for comparisons at 6 months: control F versus *Sfl1-Rspo1^{GOF}* F, *P*<0.0001; control M versus *Sfl1-Rspo1^{GOF}* M, *P*=0.9500; *Sfl1-Rspo1^{GOF}* F versus *Sfl1-Rspo1^{GOF}* M, *P*<0.0001. Adjusted *P*-values for comparisons at 12 months: control F versus *Sfl1-Rspo1^{GOF}* F, *P*=0.0008; control M versus *Sfl1-Rspo1^{GOF}* M, *P*=0.0144; *Sfl1-Rspo1^{GOF}* F versus *Sfl1-Rspo1^{GOF}* M, *P*=0.4853. ns, not significant; **P*<0.05; ****P*<0.001; *****P*<0.0001. (E) H&E staining of adrenals from 6-week-old mice. Scale bars: 100 μ m (for insets, 20 μ m). (F) Immunofluorescence staining for tyrosine hydroxylase (TH, marker of the adrenal medulla) and 3 β HSD (marker of steroidogenic cells), using adrenal sections from 6-week-old mice. Note that the size of the scale bar is different for each picture. Scale bar: 500 μ m (for insets, 100 μ m). C, cortex; X, X-zone; M, medulla; D, degeneration.

Strikingly, sex was responsible for 26.3% of the variation in gene expression patterns among our experimental groups (Fig. 2A). To gain insights into the molecular changes occurring in different subgroups, we next performed gene set enrichment analysis (GSEA) using the Molecular Signature Database (Broad Institute, Cambridge, MA, USA). Genes enriched in *Sfl1-Rspo1^{GOF}* animals of both sexes compared to controls (corresponding to cluster 1 of the heatmap in Fig. S4B) were related to β -catenin upregulation (Fevr et al., 2007; Sansom et al., 2007) or targets of the β -catenin-associated transcription factor LEF1 (Xie et al., 2005), a finding consistent with an hyperactivation of canonical WNT signaling by *Rspo1*. Genes specifically upregulated in female *Rspo1^{GOF}* adrenals (corresponding to cluster 3 of the heatmap in Fig. S4B) were found to be primarily related to cell cycle regulation, DNA replication and repair, and cell division (Fig. 2B). A more in-depth GSEA revealed that targets of transcription factors belonging to the E2F family and the DREAM complex (Fischer et al., 2016), critical repressors of cell cycle genes participating in the G1/S and G2/M transitions, were specifically upregulated in female *Sfl1-Rspo1^{GOF}* adrenals (Fig. 2C). On the contrary, genes highly expressed in male *Sfl1-Rspo1^{GOF}* adrenals (corresponding to cluster 2 of the heatmap in Fig. S4B) were associated with the regulation of the immune system and defense response (Fig. 2B). Moreover, an unbiased comparison of differentially regulated genes between male and female *Sfl1-Rspo1^{GOF}* adrenals via GSEA confirmed that 'DNA replication' and 'immune response' were among the top enriched pathways in female and male *Sfl1-Rspo1^{GOF}* adrenals, respectively (Fig. S4C). Of note, GSEA revealed a downregulation of catecholamine secretion in *Sfl1-Rspo1^{GOF}* adrenals compared to controls, probably reflecting the fragmentation of the medulla that we observed in our histological analysis (Fig. 1F).

To confirm the conclusions drawn from the mRNA sequencing experiment, we analyzed DNA replication in the adrenal cortex at 6 weeks of age via bromodeoxyuridine (BrdU) incorporation (Fig. 2D,E). No differences in proliferation between control and GOF adrenals were observed in the outer cortex, which makes up the proliferating zone under wild-type circumstances. However, proliferation was dramatically increased in the inner cortex of *Sfl1-Rspo1^{GOF}* females, which mostly consists of quiescent cells in the control animals. Surprisingly, no increase was observed in male *Sfl1-Rspo1^{GOF}* adrenals. Ordinary two-way ANOVA analysis confirmed the interactive effect of sex and *Rspo1* overexpression in regulating proliferation in the inner cortex (*P*=0.0028). Sex-specific proliferation was not observed before puberty, as male and female GOF adrenals both showed increased proliferation rates during embryogenesis (Fig. S5A,B), whereas ordinary two-way ANOVA analysis showed the absence of interactive effect between sex and the presence of the transgene at this early stage (*P*=0.8311).

Previous work from our group has shown the dominant role of RSPO3 over RSPO1 in the mouse adrenal cortex. Even though *Rspo3* deletion led to cortical atrophy both during development and in adulthood, *Rspo1* deletion did not produce an apparent defect (Vidal et al., 2016). In order to test whether the phenotype we observed was specific to *Rspo1^{GOF}*, we analyzed the effect of ectopic *Rspo3* expression in the adrenal cortex, taking advantage of a previously published *Rspo3^{GOF}* allele in the *Rosa26* locus (Hilkens et al., 2017) and the *Sfl1-Cre* system (Fig. S6A). *Rspo3* overexpression phenocopied our *Sfl1-Rspo1^{GOF}* model in terms of sex-specific hyperplasia and ectopic proliferation at 6 weeks of age (Fig. S6B,C). However, we were not able to compare the two models directly because the expression of the *Rspo3* transgene was not uniform (Fig. S6D). Thus, we conclude that overexpression of either R-spondin affects the adrenal cortex in the same manner.

Male *Rspo1^{GOF}* adrenals display abnormal macrophage accumulation

Because our transcriptomic analysis revealed an enrichment for immune-related genes among the cluster of genes specifically upregulated in male *Rspo1^{GOF}* adrenals, we examined the expression of macrophage markers by immunofluorescence staining. CD68 represents a marker of inflammation abundantly expressed in macrophages and is also detected in other cell types of the myeloid lineage (Chistiakov et al., 2017). CD68 is expressed in wild-type adrenals at 6 weeks of age at the border between the cortex and the medulla or the X-zone (Fig. 2F). By contrast, CD68 marked small cells scattered around the cortex in the hyperplastic *Sfl1-Rspo1^{GOF}* female adrenals of the same age, whereas in male *Sfl1-Rspo1^{GOF}* adrenals, CD68 marked cells increasing in size that adopted a 'foamy' morphology, fused and contributed to the formation of the degenerative lesions (Fig. 2F). Several genes expressed in macrophages and monocytes, as well as pan-immune cell markers, were upregulated in male *Sfl1-Rspo1^{GOF}* adrenals (Fig. S7A). Moreover, IBA1 (*Aif1*), a macrophage marker that has been shown to be induced in *Star* knockout animals (Ishii et al., 2012), was strongly expressed in male *Sfl1-Rspo1^{GOF}* adrenals, but not in their female counterparts (Fig. S7B). On the contrary, male-specific foamy cell formation was not observed when *Rspo1* overexpression was activated by the adrenal cortex-specific aldosterone synthase (AS) *Cyp11b2-Cre* line (Freedman et al., 2013) (more details about this genetic model are provided in the 'AR signaling determines sexual dimorphism in *Rspo1*GOF adrenals' section) (Fig. S7C). The discrepancy can be explained by the slower rate of recombination of *Cyp11b2-Cre* (5 weeks of age for the whole adrenal cortex to express the transgene) compared to that of *Sfl1-Cre*

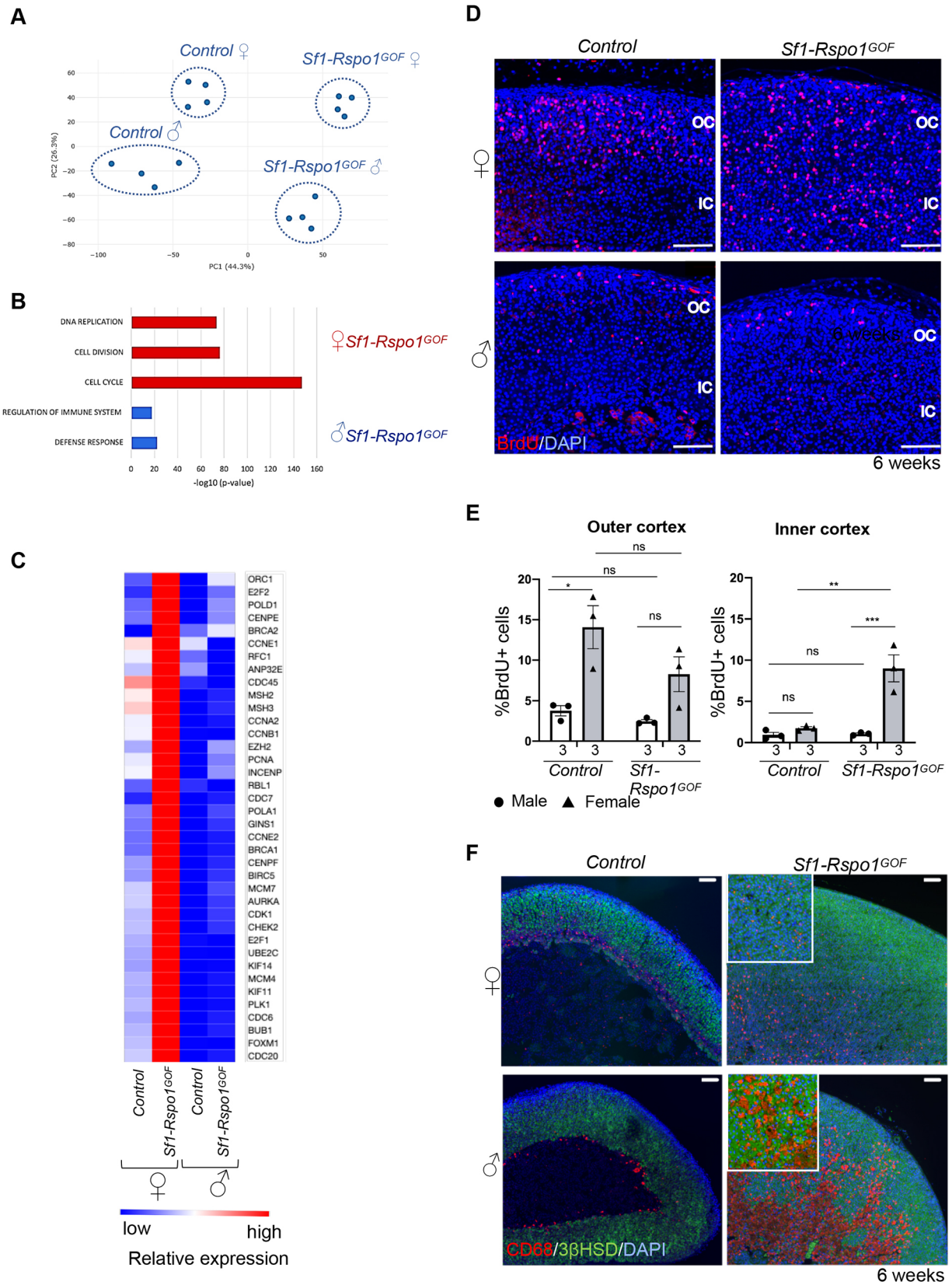


Fig. 2. See next page for legend.

(the transgene is expressed already during embryonic life). Therefore, our results indicate that the sex-specific degeneration has its origins in early, possibly embryonic, dysregulation. Overall, our data suggest that

male *Sf1-Rspo1*^{GOF} adrenals develop a sex-specific inflammatory profile, characterized by increased presence of monocytes and macrophages, that culminates in cortical thinning with increased age.

Fig. 2. Transcriptomic analysis of *Sfl1-Rspo1^{GOF}* adrenals during puberty reveals sex-specific regulation of cell cycle and immune responses. (A) Principal component analysis (PCA) plot of gene expression data in control and *Sfl1-Rspo1^{GOF}* male versus female adrenals during puberty (4 weeks of age). Each dot corresponds to an independent biological replicate. (B) Top enriched Gene Ontology terms in the clusters representing genes that are highly expressed in male or female *Sfl1-Rspo1^{GOF}* adrenals compared to those from the other experimental groups. *P*-value indicates statistical significance. (C) Heatmap representation of relative differences in expression of proliferation-related genes among experimental groups. Relative expression among the groups is indicated by the color code. The expression of all genes shown here is known to be induced during either the G1/S or the G2/M transitions of the cell cycle. (D) Representative immunofluorescence images for BrdU. Scale bars: 100 μ m. OC, outer cortex; IC, inner cortex. (E) BrdU proliferation analysis shown as mean percentage of proliferating cells over total number of cells in the adrenal cortex of 6-week-old mice (error bars represent s.e.m.). The numbers below the graph columns represent number of samples in each group (*n*=3). The area close to the capsule (outer cortex) is distinguished from the deeper layers (inner cortex). Statistical analysis was performed using ordinary two-way ANOVA followed by Tukey's multiple comparisons test. Adjusted *P*-values for the outer cortex graph: control females (F) versus *Sfl1-Rspo1^{GOF}* F, *P*=0.1623; control F versus control males (M), *P*=0.0128; *Sfl1-Rspo1^{GOF}* F versus *Sfl1-Rspo1^{GOF}* M, *P*=0.1638; control M versus *Sfl1-Rspo1^{GOF}* M, *P*=0.9506. Adjusted *P*-values for the inner cortex graph: control F versus *Sfl1-Rspo1^{GOF}* F, *P*=0.0013; control F versus control M, *P*=0.8967; *Sfl1-Rspo1^{GOF}* F versus *Sfl1-Rspo1^{GOF}* M, *P*=0.0007; control M versus *Sfl1-Rspo1^{GOF}* M, *P*=0.9996. ns, not significant; **P*<0.05; ***P*<0.01; ****P*<0.001. (F) Immunofluorescence staining for CD68 (marker of murine macrophages) and 3 β HSD (marker of steroidogenic cells) using adrenal sections from 6-week-old mice. Scale bars: 100 μ m.

Sex-specific pattern of canonical WNT signaling activation in *Rspo1^{GOF}* adrenals

In order to identify the cause of sexual dimorphism in our model, we tested whether sex influences canonical WNT signaling activation. To focus on primary events, we chose an early timepoint (4 weeks) when sex-specific differences in proliferation start to emerge, but degeneration is not yet obvious in male adrenals. In agreement with previous research (Leng et al., 2020), β -catenin shows strong membrane immunoreactivity in the zG but is absent in the inner cortex of control animals (apart from cells containing small spindle-like nuclei that do not have the characteristic morphology of steroidogenic cells). However, in *Sfl1-Rspo1^{GOF}* adrenals, we observed increased membrane, nuclear and perinuclear β -catenin immunoreactivity in the inner cortex, in addition to its characteristic zG pattern (Fig. 3A). To quantify this disruption of the characteristic WNT signaling gradient, we performed RNA Scope *in situ* hybridization (ISH) analysis for *Axin2* and *Wnt4*, two markers of canonical WNT signaling activation. Although *Axin2* is a well-characterized target of canonical WNT signaling (Jho et al., 2002), *Wnt4* is thought to be a driver of canonical WNT signaling in the adrenal cortex (Basham et al., 2019; Vidal et al., 2016). Consistent with previous data (Basham et al., 2019), the expression of these two genes follows a gradient of diminishing expression from the outer to the inner cortex in control animals, which was disrupted in our GOF model (Fig. 3B,C). Interestingly, the expression of these two genes became sexually dimorphic in *Sfl1-Rspo1^{GOF}* adrenals, with *Axin2* expression being increased in males (reaching statistical significance in the outer cortex) and *Wnt4* expression being increased in females (reaching statistical significance in the inner cortex) (Fig. 3D,E).

AR signaling determines sexual dimorphism in *Rspo1^{GOF}* adrenals

To explain sexual dimorphism in adrenocortical hyperplasia, it is essential to dissect the role of sex hormones versus the role of sex

chromosomes. We took advantage of a sex reversal model in which constitutive ectopic expression of a *Wtl-Sox9* gene in XX gonads leads to the development of testes (Vidal et al., 2001) (Fig. 4A). Sex-reversed *Sfl1-Rspo1^{GOF}* males [*Gt(Rosa)26Sor^{cCAG-Rspo1⁺}*; *Sfl1-cre^{Tg/0}*; *Wtl-Sox9^{Tg/0}* XX] displayed significantly lower normalized adrenal weight than *Sfl1-Rspo1^{GOF}* females [*Gt(Rosa)26Sor^{cCAG-Rspo1⁺}*; *Sfl1-cre^{Tg/0}* XX] (Fig. 4B) and developed vacuolated cells in the inner cortex at 6 weeks of age (Fig. 4C), thus phenocopying XY *Sfl1-Rspo1^{GOF}* male adrenals. These data indicate that gonadal rather than chromosomal sex is responsible for the sexual dimorphism.

We have shown previously that androgens can suppress progenitor proliferation during normal adrenal cortex homeostasis (Grabek et al., 2019). To test whether androgens would also modify female-specific hyperplasia in our mouse model, we chose to treat *Sfl1-Rspo1^{GOF}* female mice daily with the androgen DHT during puberty (3-6 weeks of age) (Fig. 4D). Expression analysis revealed a slight reduction of the AR gene (*Ar*), as well as a dramatic increase in the expression of *Susd3*, a putative androgen-responsive gene in the adrenal cortex (as suggested by our RNA-seq data and previous transcriptomic analyses; El Wakil et al., 2013) (Fig. S8B). Moreover, DHT treatment dramatically reduced normalized adrenal weight and proliferation levels in the adrenal cortex (Fig. 4D,E) but did not lead to histological changes such as cytoplasmic vacuolization (Fig. S8A). The reduction of proliferation levels in DHT-treated animals was accompanied by a reduction in expression levels of genes associated with the G1/S transition of the cell cycle (*E2f8*, *Pcna*, *Cdc6* and *Polal*) (Fischer and Müller, 2017) (Fig. 4F). However, the expression of cell cycle genes that are also known β -catenin targets (*Cnd1* and *Myc*) (Shtutman et al., 1999; Van de Wetering et al., 2002) did not show statistically significant changes after treatment, suggesting that the effect of the androgens on cell cycle progression is not due to direct regulation of β -catenin targets (Fig. S8B). Furthermore, DHT treatment led to an increase in *Axin2* expression levels and to a decrease in *Wnt4* expression levels (Fig. S8B), similarly to what RNA Scope ISH analysis suggested regarding the effect of sex on the expression of WNT-related genes (Fig. 3C,E). Interestingly, long-term DHT treatment did not cause consistent changes in the subcellular localization of β -catenin in the inner cortex (Fig. S8C).

Adrenal cortex homeostasis depends on complex endocrine interactions with the pituitary-hypothalamic axis and the gonads (Goel et al., 2014). Having established a role for DHT in suppressing hyperplasia, we asked whether this effect is direct or involves feedback loops via other organs. To answer this question, we took advantage of a conditional knockout (KO) allele for *Ar* (De Gendt et al., 2004) that we activated simultaneously with the *Rspo1* transgene. To exclude extra-adrenal effects, we employed the adrenal cortex-specific AS *Cyp11b2-Cre* line (Freedman et al., 2013) (Fig. 5A) that becomes activated in the zG at birth and – owing to the centripetal displacement of cortical cells – leads to recombination throughout the cortex by approximately 5 weeks of age. Given the slower recombination rate compared to that of *Sfl1-Cre*, we analyzed adrenals at 20 weeks of age. Similarly to *Sfl1-Cre*, *Cyp11b2-Cre* activation of *Rspo1(AS-Rspo1^{GOF})* resulted in female adrenal hyperplasia, whereas growth of the male adrenals remained comparable to that of wild-type controls (Fig. 5B). Strikingly, simultaneous deletion of the *Ar* allele caused a significant increase of male adrenals to a weight comparable to that found in female counterparts (Fig. 5B). Moreover, male *AS-Rspo1^{GOF}/Ar KO* and female *AS-Rspo1^{GOF}* adrenals appeared similar on the histological level, characterized by cortical hyperplasia (Fig. S9A). BrdU-based

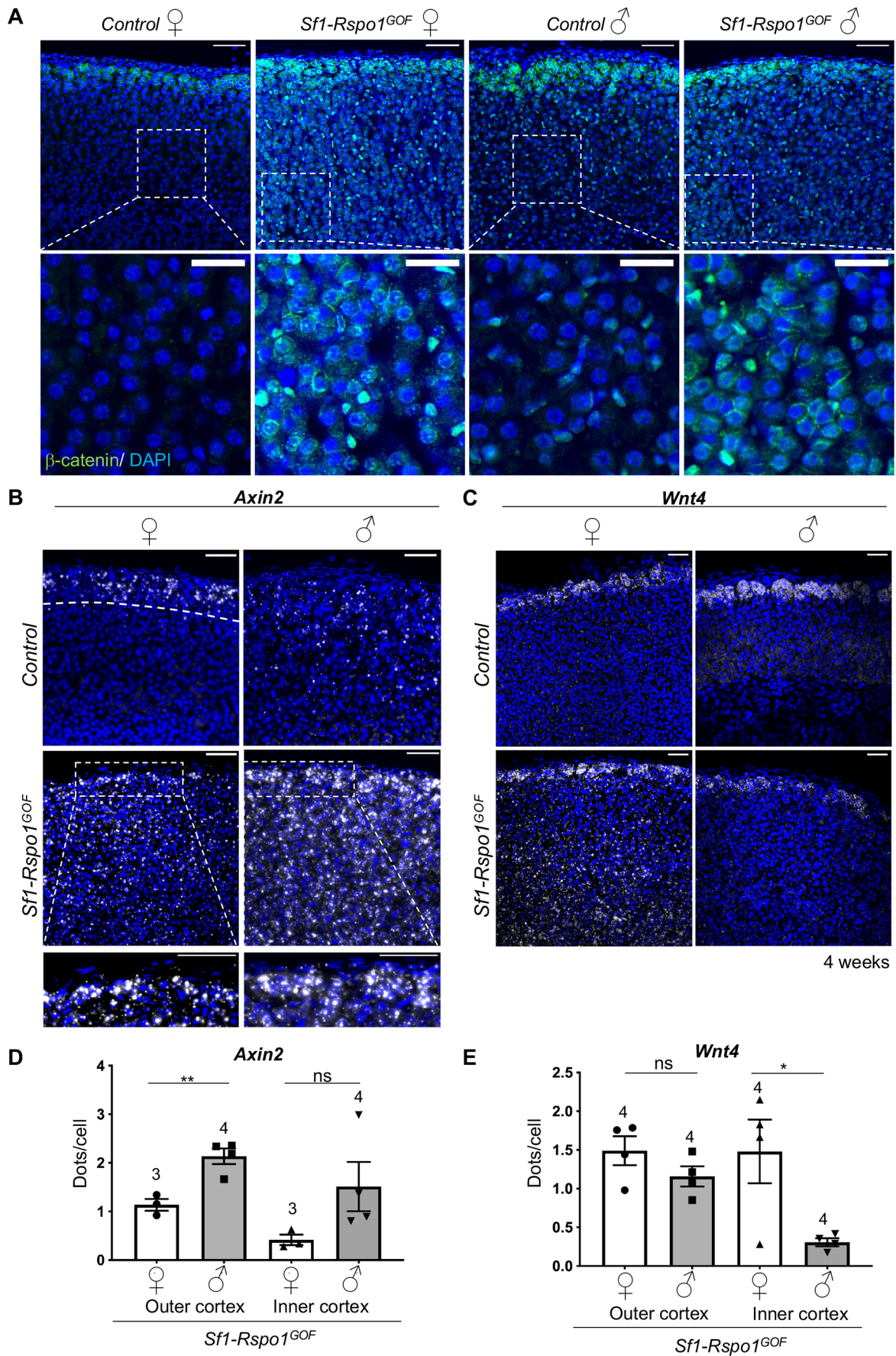


Fig. 3. See next page for legend.

Fig. 3. *Rspo1* overexpression induces the expansion of canonical WNT activity zone in the adrenal cortex in a sexually dimorphic manner.

(A) Immunofluorescence staining for β -catenin using adrenal sections from 4-week-old mice. Scale bar: 50 μ m (top panels); 20 μ m (bottom panels). (B,C) *In situ* hybridization using the RNA Scope technology for *Axin2* (B), a target of canonical WNT signaling, and *Wnt4* (C) at 4 weeks of age. Insets represent high-power images of the outer cortex in GOF animals. The outer cortex is denoted by a dotted line in B (female control; top left panel). Scale bars: 50 μ m. (D,E) Graphs showing the mean number of *Axin2* (D) and *Wnt4* (E) transcripts per cell in the outer cortex or inner cortex, based on RNA Scope-based detection on adrenal sections from 4-week-old mice (error bars represent s.e.m., whereas each dot represents an independent biological replicate). The numbers above the graph columns represent number of samples in each group (*n*). Statistical analysis was performed using unpaired two-tailed *t*-test. *P*-value comparing male versus female outer cortex for *Axin2*=0.0058. *P*-value comparing male versus female inner cortex=0.1302. *P*-value comparing male versus female outer cortex for *Wnt4*=0.1963. *P*-value comparing male versus female inner cortex=0.0301. ns, not significant; **P*<0.05; ***P*<0.01.

analysis confirmed an increase in proliferation in male *Rspo1*^{GOF}/*Ar* KO adrenals, particularly in the inner cortex. The observed variability among different animals (Fig. 5C,D) is likely due to incomplete deletion of the *Ar* allele in clusters of adrenocortical cells (Fig. S9B). Surprisingly, *Ar* deletion led to a mild increase of β -catenin accumulation in cells in certain areas of the inner cortex of *AS-Rspo1*^{GOF} male adrenals (Fig. S9C). However, quantification of *Axin2* expression in the outer and inner cortex using RNA Scope ISH (Fig. S9D) revealed no significant changes, suggesting that *Ar* deletion does not translate into a change of transcriptional activity of β -catenin. Taken together, our results demonstrate that androgens act directly on adrenocortical cells by engaging their cognate receptor and cause proliferation arrest, contributing to a differential susceptibility to adrenocortical hyperplasia among the sexes (Fig. 6).

DISCUSSION

Canonical WNT/ β -catenin signaling gradients determine a plethora of processes, ranging from embryonic development to the maintenance of adult stem cell niches, whereas their dysregulation is linked to carcinogenesis in humans (Nusse and Clevers, 2017). High β -catenin levels in the zG of the mouse adrenal cortex, supported by secreted R-spondins, are paramount to maintaining regular renewal and zonation (Kim et al., 2008; Vidal et al., 2016). Here, we report adrenal hyperplasia of the zF owing to R-spondin overexpression and mild WNT signaling activation. Although our model phenotypically resembles the effects of *Znrf3* deletion described before (Basham et al., 2019), we also describe a striking, androgen-dependent sexual dimorphism in phenotypic development, which was not reported in this earlier study. Notably, the two studies corroborate the tied role of R-spondin ligands and the ZNRF3 ubiquitin ligase in maintaining the WNT/ β -catenin signaling gradient and localized proliferation in the adrenal cortex.

We found that immune system activation and abnormal proliferation, two major pillars of tumorigenesis, are regulated in a sex hormone-specific manner in *Rspo1*^{GOF} mice. Indeed, males displayed the recruitment of macrophages, monocytes and dendritic cells when *Sfl-Cre* was used to induce *Rspo1* overexpression (*Sfl-Rspo1*^{GOF}). On the histological level, this recruitment manifested as foamy cell formation, cytoplasmic vacuolization and tissue degeneration. Remarkably, we did not observe the same male-specific foamy macrophage formation in the *AS-Rspo1*^{GOF} model. This discrepancy might reflect the differential rates of Cre

activation, as *Sfl-Cre* is active during embryogenesis, whereas the *AS-Cre* line results in cortex-wide recombination only at 5 weeks of age (Freedman et al., 2013). We can hypothesize that embryonically derived macrophages are involved, such as the CX3CR1⁺ population, recently demonstrated by a study analyzing sex-specific differences in adrenal cortex macrophage distribution and expression profile (Dolfi et al., 2022). Alternatively, macrophage recruitment could result from extra-adrenal *Rspo1* overexpression, as *Sfl-Cre* is also expressed in other endocrine organs, such as the gonads. We consider this scenario less likely, as plasma levels of androgens do not differ significantly between control and *Sfl-Rspo1*^{GOF} animals, thus excluding the hypothesis that excess of gonadal androgens induces macrophage recruitment in males.

Recently, an independent study reported a male-specific, proinflammatory environment and abundant recruitment of macrophages in the *Znrf3* knockout adrenal cortex in response to the appearance of senescent cortical cells. The authors suggest that androgen-dependent macrophage recruitment may be a significant contributor to female bias in ACC (Wilmouth et al., 2022). We did not observe histological changes consistent with macrophage recruitment after DHT treatment, but this may be due to the relatively short timeframe of androgen treatment in our study. Of note, the finding of macrophage infiltration upon *Rspo1* overexpression and *Znrf3* deletion is contrary to studies in other systems in which WNT/ β -catenin activation has been reported to favor exclusion of infiltrating immune cells from the tumor microenvironment (Muto et al., 2023). Although macrophage recruitment is likely to contribute to the degenerative phenotype in male mice, androgen-induced proliferation arrest appears to be cell intrinsic and independent of macrophage activity. Indeed, deletion of *Ar* induces hyperproliferation in our *AS-Rspo1*^{GOF} mice, a model that does not show macrophage recruitment.

However, a high proliferation index is an important feature of ACC, associated with malignant rather than benign tumors and worse prognosis (Crona and Beuschlein, 2019). Moreover, dysregulation of WNT/ β -catenin signaling and cell cycle regulation [via the p53/retinoblastoma-associated protein (RB1) axis] are significant hallmarks of ACC and the pathways most frequently affected by driver mutations (Assié et al., 2014; Zheng et al., 2016). In this context, our findings can contribute to a greater understanding of sex bias in ACC frequency and the development of personalized therapies. In future studies, it will be important to test whether androgen administration in the context of other ACC models (Borges et al., 2020) also suppresses proliferation and tumor growth. Of note, it has been described that DHT treatment of human ACC cells leads to growth arrest (Rossi et al., 1998).

Androgens are potent suppressors of the hypothalamic-pituitary-adrenal axis at the level of the hypothalamus and the pituitary gland, which in turn regulate corticosterone production by the adrenal cortex (Seale et al., 2004). Distinguishing direct versus indirect effects of sex hormones in gonadectomy and DHT-treatment experiments has therefore been difficult. We show here that removing the cognate DHT receptor from adrenocortical cells (*Ar* deletion) renders male adrenals susceptible to hyperplasia and hyperproliferation and abolishes sexual dimorphism. Thus, this is the first report of AR signaling directly suppressing proliferation in the adrenal cortex. Of note, it has been shown before that AR signaling influences adrenal weight and X-zone regression (Gannon et al., 2019).

Although the genetic evidence for suppression of steroidogenic cell proliferation by AR is striking, the molecular mechanisms underlying this process are less clear. Direct antagonism between

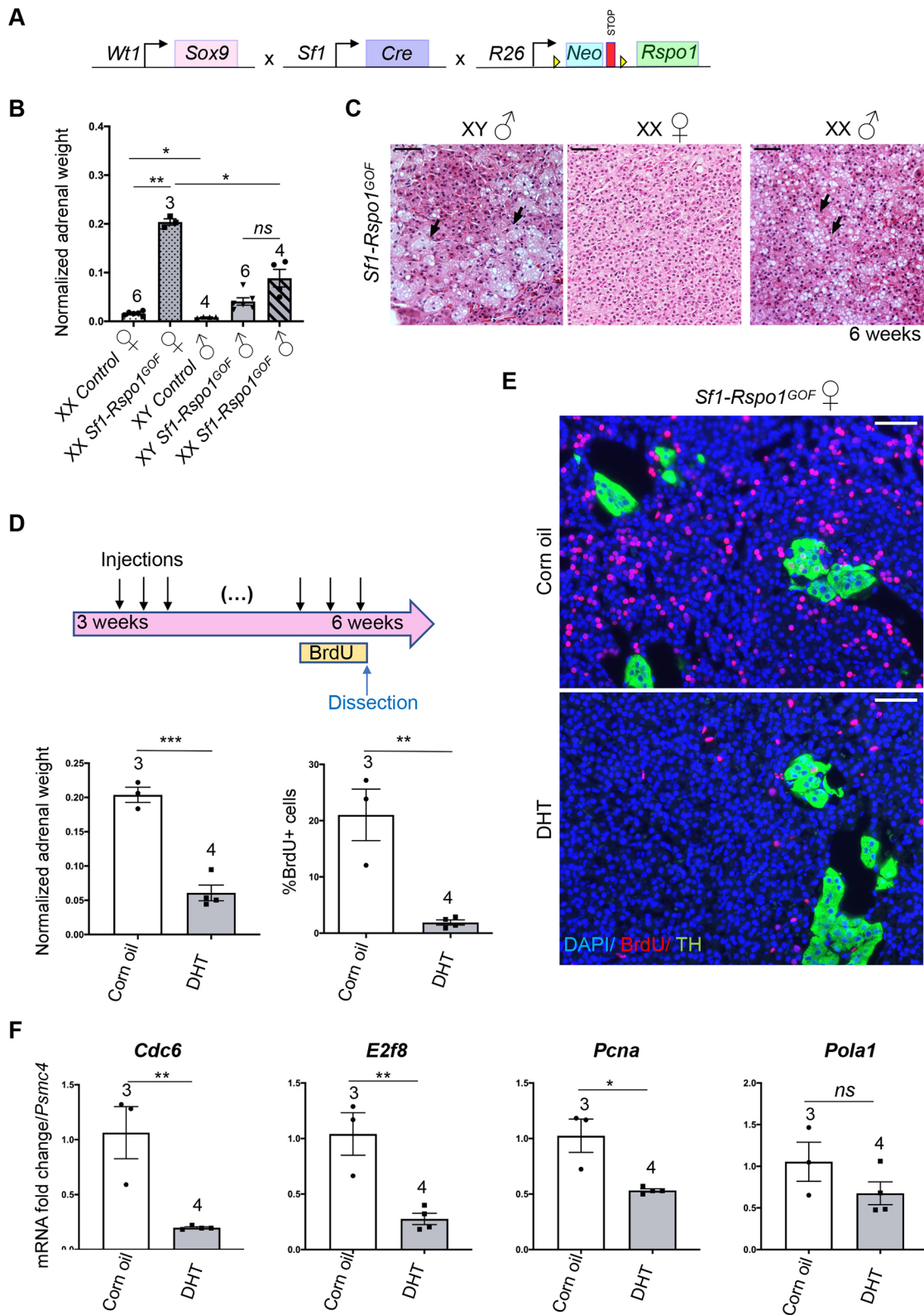


Fig. 4. See next page for legend.

AR and WNT/ β -catenin signaling has been suggested before for epidermal stem cells (Kretzschmar et al., 2015) and prostate cancer cells (Mulholland et al., 2003). In our model, we did not find evidence for a sex-specific global reduction of β -catenin signaling in male compared to female adrenals. On the contrary, *Axin2*

expression – a recognized marker of WNT/ β -catenin signaling – was reproducibly increased in the inner cortex of males compared to females and was induced following DHT treatment. This observation agrees with the work from Dumontet et al. (2018), which suggested that androgens positively affect WNT signaling in

Fig. 4. Sexually dimorphic response to RSPO1 overexpression is caused by androgens.

(A) Schematic representation of the genetic strategy to combine RSPO1 overexpression in steroidogenic tissues with female-to-male sex-reversal caused by ectopic SOX9 expression under control of a *Wt1* regulatory sequence. (B) Mean adrenal weight normalized to whole-body weight at 6 weeks. 'XX' and 'XY' denote sex chromosomes and 'XX δ ' indicates sex-reversed *Tg(Wt1-Sox9)^{Tg/0}* mice. Statistical analysis was performed with one-way Welch's ANOVA followed by Dunnett's T3 multiple comparisons test. Adjusted *P*-values: XX control F versus XX *Sfl1-Rspo1^{GOF}* F, *P*=0.0048; XX control F versus XY control M, *P*=0.0367; XX *Sfl1-Rspo1^{GOF}* F versus XX *Sfl1-Rspo1^{GOF}* M, *P*=0.0231. (C) H&E staining on adrenal sections from 6-week-old XY and XX *Sfl1-Rspo1^{GOF}* male mice. Black arrows point to vacuolated cells that form degenerative lesions. Scale bars: 50 μ m. (D) Female *Sfl1-Rspo1^{GOF}* mice were treated with DHT or corn oil daily for 3 weeks during puberty. Graphs represent mean adrenal weight normalized to total body weight (bottom left; *P*=0.0003) and percentage of proliferating cells (BrdU*) in the adrenal cortex (bottom right; *P*=0.0043). Statistical analysis was conducted using unpaired two-tailed *t*-test. (E) Representative immunofluorescence images for BrdU and TH (marker of the medulla). Scale bars: 50 μ m. (F) RT-qPCR analysis of the expression of genes related to the G1/S cell cycle transition. Graphs represent mean fold-change in expression comparing corn oil to DHT treated adrenals (normalized to *Psmc4* expression). Statistical analysis was conducted with unpaired *t*-test. *P*-values: 0.1964 (*Pola1*), 0.0066 (*E2f8*), 0.0073 (*Cdc6*) and 0.0117 (*Pcna*). DHT: dihydrotestosterone. All error bars represent s.e.m. The numbers above the graph columns represent number of samples in each group (*n*). ns, not significant; **P*<0.05; ***P*<0.01; ****P*<0.001.

the adrenal cortex, thus counteracting PKA signaling and cortical cell turnover. This molecular action is believed to contribute to the female susceptibility to Cushing's syndrome. However, whether AR is directly involved in this phenomenon is questionable, as we did not find markedly altered *Axin2* expression following *Ar* deletion in the male GOF adrenal cortex.

Another possibility is that AR suppresses transcription of cell cycle genes independently of WNT signaling. Indeed, although we found that the expression of several G1/S cell cycle transition genes was repressed by DHT treatment, these known targets of β -catenin remained almost stable. Interestingly, it has already been reported that AR acts as a transcriptional repressor for a subset of DNA replication genes by recruiting RB1 to their promoters (Gao et al., 2016).

The finding that AR suppresses proliferation in the adrenal cortex might seem surprising, given the well-characterized association of AR with prostate growth, benign prostate hyperplasia and prostate tumorigenesis (Dai et al., 2017). However, even in prostate cancer, AR can have opposing effects on cell cycle regulation, depending on ligand concentration, duration of treatment and the extent of GOF alterations in AR signaling in the context of malignant transformation (Chatterjee et al., 2019; Gao et al., 2016; Litvinov et al., 2006). Moreover, it has been suggested that AR acts as a tumor suppressor in the context of breast cancer (Hickey et al., 2021). Our study contributes to understanding of AR signaling complexity and tissue specificity and highlights one prominent cause of sexual dimorphism in a non-reproductive organ. Further work will be required to delineate the precise mechanistic underpinnings of androgen-specific suppression of proliferation in the context of the adrenal cortex.

MATERIALS AND METHODS

Animal husbandry and genetics

All animal work was conducted according to national and international guidelines and approved by the local ethical committee [Comité Institutionnel d'Éthique Pour l'Animal de Laboratoire (CIEPAL): APAFIS#6001-201606281711255 v6, APAFIS#14137-2018030216239792 v1] and the French Ministry of Agriculture. The mouse strains (*Mus musculus*) used in this study have been reported previously: *Rspo1^{GOF}* (De Cian et al., 2017; Rocha et al., 2015), *Sfl1-Cre* (Bingham et al., 2006), *Wt1-Sox9* (Vidal

et al., 2001), *Rspo3^{GOF}* (Hilkens et al., 2017), *Cyp11b2-Cre* (Freedman et al., 2013) and *Ar^{lox}* (De Gendt et al., 2004). Mice heterozygous for the *Rspo1^{GOF}* allele and the *Sfl1-Cre* allele are referred to as '*Sfl1-Rspo1^{GOF}*' [*Gt(Rosa)26Sor^{cCAG-Rspo1/+}; Sfl1-Cre^{Tg/0}*], whereas mice with genotypes that do not permit the expression of the GOF allele are referred to as controls [*Gt(Rosa)26Sor^{+/+}; Sfl1-Cre^{Tg/0}*, *Gt(Rosa)26Sor^{+/+}; Sfl1-Cre^{0/0}* or *Gt(Rosa)26Sor^{cCAG-Rspo1/+}; Sfl1-Cre^{0/0}*]. The expression of a *Wt1-Sox9* allele distinguishes sex-reversed *Sfl1-Rspo1^{GOF}* males [*Gt(Rosa)26Sor^{cCAG-Rspo1/+}; Sfl1-Cre^{Tg/0}; Wt1-Sox9^{Tg/0} XX*] from *Sfl1-Rspo1^{GOF}* females [*Gt(Rosa)26Sor^{cCAG-Rspo1/+}; Sfl1-Cre^{Tg/0}; Wt1-Sox9^{0/0} XX*] and males [*Gt(Rosa)26Sor^{cCAG-Rspo1/+}; Sfl1-Cre^{Tg/0}; Wt1-Sox9^{0/0} XY*]. Mice heterozygous for the *Rspo1^{GOF}* allele and *Cyp11b2* (aldosterone synthase)-*Cre* are referred to as '*AS-Rspo1^{GOF}*' [*Gt(Rosa)26Sor^{cCAG-Rspo1/+}; Cyp11b2^{Cre/+}*], compared to the genotype that does not permit expression of the GOF allele, referred to as control [*Gt(Rosa)26Sor^{+/+}; Cyp11b2^{+/+}*]. When the gene encoding for AR is deleted in males, mice are referred to as '*AS-Rspo1^{GOF}/Ar KO*' [*Gt(Rosa)26Sor^{cCAG-Rspo1/+}; Cyp11b2^{Cre/+}; Ar^{lox/Y}*]. Mouse lines were maintained on a mixed genetic background. Both males and females were analyzed at various ages as indicated in the main text, whereas littermates were preferentially compared.

Immunofluorescence and histology

For immunofluorescence and H&E analysis of paraffin-embedded samples, mouse left adrenal tissues were fixed overnight at 4°C with 4% paraformaldehyde, progressively dehydrated and paraffin embedded. For H&E staining, sections of 5 mm were rehydrated and stained with Eosin and Mayer's Hematoxylin (3 min each), before being dehydrated again and mounted using an anhydrous mounting medium. Carcinoma and adenoma formation was verified by expert pathologists. For immunofluorescence, 5 mm sections were unmasked with PT Link (Dako Agilent Pathology Solutions) at pH 6 or 9. Sections were blocked for 1 h with 10% normal donkey serum (Jackson ImmunoResearch), 3% bovine serum albumin (BSA; Sigma-Aldrich) and 0.1% Tween-20 (Sigma-Aldrich). Primary antibodies were applied overnight at 4°C diluted in 3% normal donkey serum, 3% BSA and 0.1% Tween-20 as explained in Table S2. The next day, sections were incubated at room temperature with secondary antibodies donkey anti-rabbit Alexa Fluor 647, donkey anti-goat Alexa Fluor 555, donkey anti-mouse Alexa Fluor 555, donkey anti-rabbit Alexa Fluor 555 and donkey anti-mouse Alexa Fluor 647 diluted 1:400 in PBS (see Table S2). Sections were then mounted in antifade mounting medium with DAPI (Vectashield). The Mouse-on-Mouse immunodetection kit (Vector Laboratories) was used to improve the signal for mouse primary antibodies according to the manufacturer's instructions. For anti-AR and anti-IBA1 immunohistochemistry, sections were incubated with biotinylated donkey anti-rabbit secondary antibodies (see Table S2) and the signal was revealed using the Vectastain Elite ABC-HRP peroxidase kit and the ImmPACT NovaRED HRP substrate (Vector Laboratories). Counterstaining was performed using 50% Harris Hematoxylin for 30 s, followed by incubation in 0.1% sodium bicarbonate solution for 1 min at room temperature. The antibodies used were all commercially available with reported validation profiles. Appropriate negative controls (without the primary antibody) were used in all immunostaining experiments.

Proliferation quantification

For proliferation quantification in the adrenal cortex, 1 mg/ml of BrdU (Sigma-Aldrich) was dissolved in autoclaved water with 2% sugar and given to mice as drinking water for 3 days. Anti-BrdU immunofluorescence was conducted as described above. Quantification was performed using the HALO image analysis platform (Indica Labs) on whole-section mosaic images obtained with the Vectra Polaris imaging system (Akoya Biosciences), excluding the medulla based on tyrosine hydroxylase (TH) staining. The number of BrdU-positive cells was expressed as the percentage of the total number of cells in each zone based on DAPI staining. When the distinction between 'outer' and 'inner' cortex is made, we refer to the zone <80 mm from the capsule and >80 mm from the capsule, respectively. At least three biological replicates (individual mice) and three non-consecutive sections for each biological replicate were analyzed.

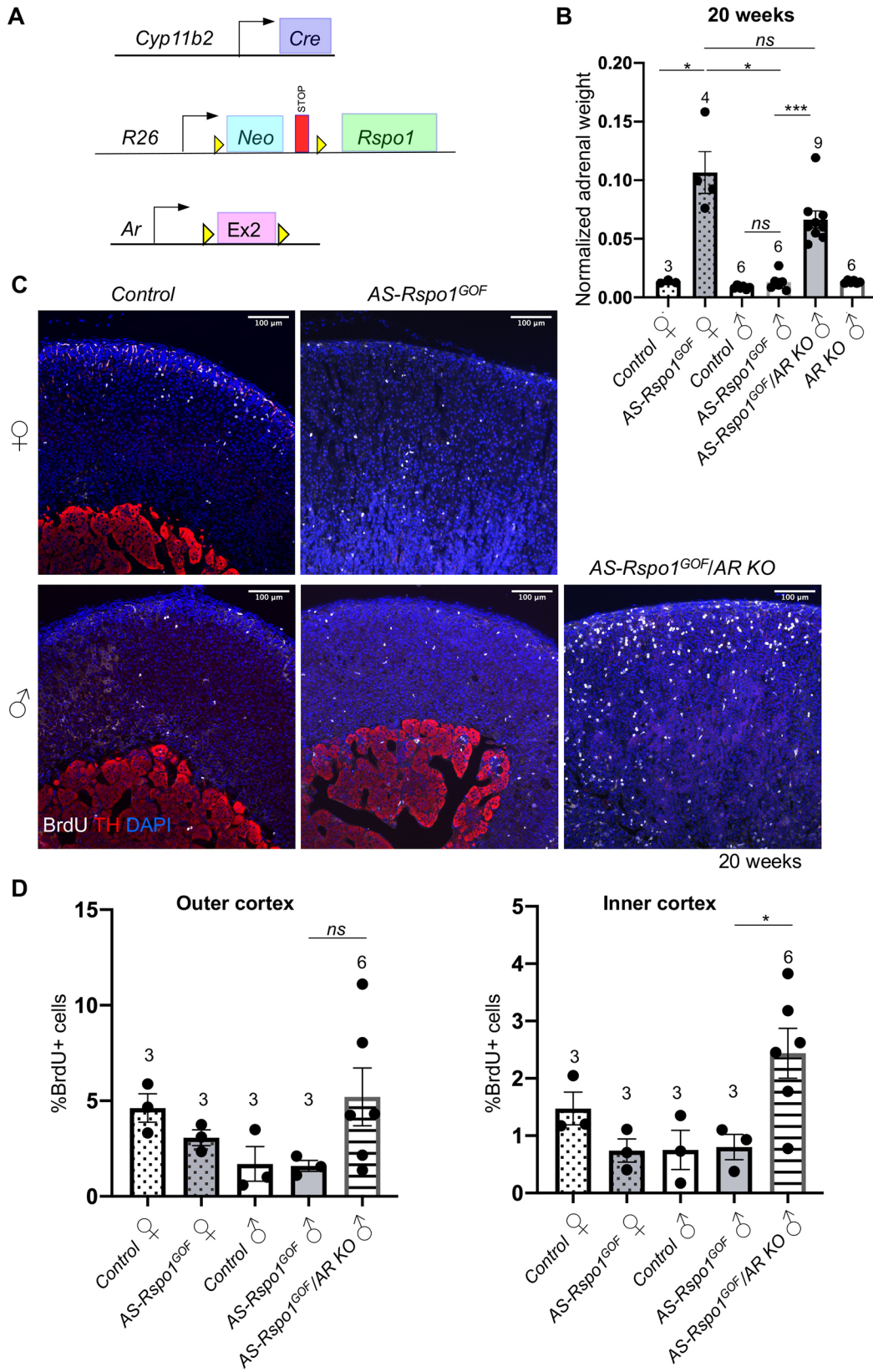


Fig. 5. See next page for legend.

Fig. 5. Androgen receptor deletion in male *AS-Rspo1^{GOF}* adrenocortical cells abolishes sexual dimorphism in the development of hyperplasia.

(A) Schematic representation of the genetic strategy to knock-out *Ar* and simultaneously overexpress *RSPO1* in adrenocortical cells using the *Cyp11b2-Cre* driver. (B) Adrenal weight normalized to body weight at 20 weeks. Statistical analysis was performed using Welch's one-way ANOVA followed by Dunnett's T3 post hoc test. Adjusted *P*-values: control F versus *AS-Rspo1^{GOF}* F, *P*=0.0454; control M versus *AS-Rspo1^{GOF}* M, *P*=0.5777; *AS-Rspo1^{GOF}* F versus *AS-Rspo1^{GOF}* M, *P*=0.0468; *AS-Rspo1^{GOF}* F versus *AS-Rspo1^{GOF}/Ar KO* M, *P*=0.3370; *AS-Rspo1^{GOF}* M versus *AS-Rspo1^{GOF}/Ar KO* M, *P*=0.0001. (C) Representative immunofluorescence images for tyrosine hydroxylase (TH) and BrdU, indicating proliferating cells. Scale bars: 100 μ m. (D) BrdU proliferation analysis shown as a percentage of proliferating cells over the total number of cells in the adrenal cortex of 20-week-old mice. The area close to the capsule (outer cortex) is distinguished from the deeper layers (inner cortex). Unpaired two-tailed *t*-test was employed to compare values for *AS-Rspo1^{GOF}* male and *AS-Rspo1^{GOF}/Ar KO* male. Adjusted *P*-values: 0.1478 (outer cortex) and 0.0410 (inner cortex). All error bars represent s.e.m. The numbers above the graph columns represent number of samples in each group (*n*). ns, not significant; **P*<0.05; ****P*<0.001.

RNA scope ISH

Adrenal sections were fixed with 4% paraformaldehyde overnight at room temperature and paraffin embedded. Fresh 5 μ m sections were subjected to single-molecule ISH using the RNA Scope 2.5 High Definition-Red assay (ACD Biotechne), according to the manufacturer's instructions. Images were acquired with a Zeiss apotome upright microscope or a Zeiss LSM NLO 780 confocal microscope. For quantification purposes, whole-section mosaic images were acquired with the Vectra Polaris imaging system (Akoya Biosciences) and quantified using the FISH Multiplex v1.1 module of the HALO image analysis platform (Indica Labs). Outer cortex represents the proliferative zone and includes the zG and 12 \pm 1% of the zF for male control animals, and 25 \pm 7% of the zF for female control animals (the zF in the females is considered shorter due to the presence of the X-zone). The inner cortex includes the rest of the zF up to the X-zone (if present) or the medulla.

Gene expression analysis

RNA was extracted from mouse right adrenals using the RNeasy mini kit (QIAGEN) according to the manufacturer's instructions. cDNA synthesis was performed using M-MLV reverse transcriptase (Invitrogen) and random primers. The obtained cDNA was used as template in a real-time quantitative PCR (RT-qPCR) reaction using the SYBR Green Master Mix (Roche) and a LightCycler 1.5 (Roche) or a QuantStudio 5 thermocycler (Applied Biosystems). Expression levels were normalized to the housekeeping gene

Psmc4, analyzed using the $2^{-\Delta\Delta Ct}$ method and presented as fold-change values compared to a reference sample. The primers used are listed in Table S1.

Hormonal treatment and analysis of hormone levels in plasma

Sfl-Rspo1^{GOF} females were injected twice daily subcutaneously with 5 α -androstano-17 β -ol-3-one (Sigma-Aldrich) (37.5 μ g in 5% ethanol and corn oil) or oil only from 3–6 weeks of age, when they were sacrificed. For the measurement of adrenal steroids in mouse plasma, 6-week-old animals were sacrificed in the morning and core trunk blood was collected in tubes containing 5 μ l of 0.5 M EDTA. The samples were centrifuged for 5 min at 4000 *g* at 4°C to separate the plasma, which was promptly frozen at –80°C until analysis. Steroid hormones were quantified by LC-MS/MS as described previously (Peitzsch et al., 2015).

RNA-seq and analysis

RNA was extracted from mouse right adrenals using the RNeasy mini kit (QIAGEN) according to the manufacturer's instructions. Four biological replicates were analyzed for each group (control male, control female, *Sfl-Rspo1^{GOF}* male and *Sfl-Rspo1^{GOF}* female). The sample quality was assessed using a Bioanalyzer 2100 (Agilent Technologies) and a RNA integrity number (RIN) cut-off value of 7.0 was applied.

Library preparation and sequencing, as well as differential expression analysis were conducted by Novogene. Briefly, library preparation was conducted using a NEBNext Ultra RNA Library Prep kit for Illumina (New England Biolabs). After cluster generation, the library preparations were sequenced on an Illumina platform and 125/150 bp paired-end reads were generated. Raw data (raw reads) of FASTQ format were firstly processed through in-house Perl scripts. In this step, clean data (clean reads) were obtained by removing reads containing adapter, reads containing poly-N and low-quality reads from raw data. All the downstream analyses were based on the clean data with high quality. The annotation was performed based on the GRCm38 genome assembly and downloaded from Ensembl. The index of the reference genome was built using Bowtie v2.2.3 and paired-end clean reads were aligned to the reference genome using TopHat v2.0.12. To count the reads numbers mapped to each gene, HTSeq v0.6.1 was used. The fragments per kilobase of transcript per million mapped reads (FPKM) value of each gene was calculated based on the length of the gene and read count mapped to this gene. Differential expression analysis was performed using the DESeq R package (v1.18.0). The resulting *P*-values were adjusted using the Benjamini and Hochberg approach for controlling the false discovery rate (FDR). Genes with an adjusted *P*-value <0.05 found by DESeq were assigned as differentially expressed.

For downstream analyses, PCA plot and heatmaps were designed using the Phantasm website tools (Kleverov et al., 2022 preprint), using

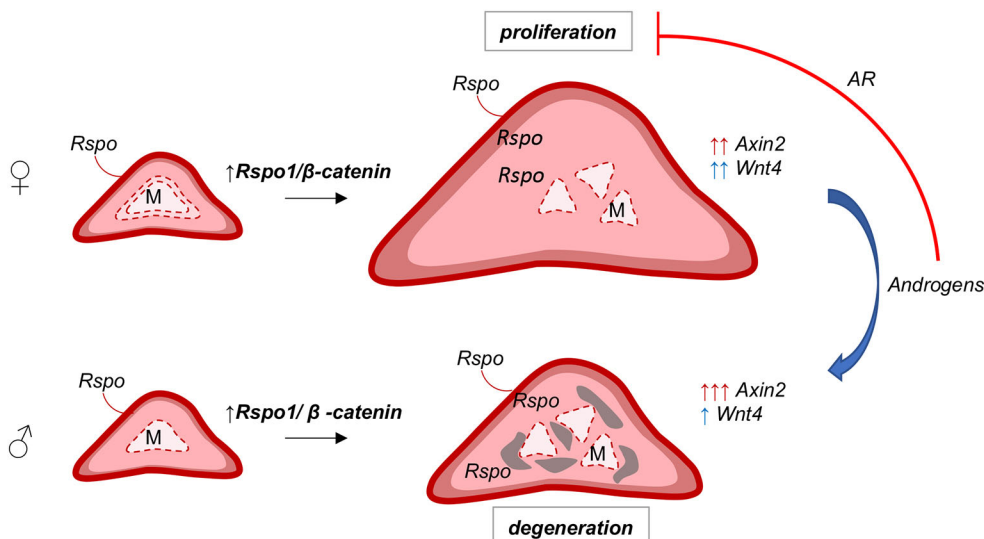


Fig. 6. Sex-specific effects of *Rspo1* overexpression in the adrenal cortex.

Localized expression of R-spondins (by the capsule) maintains high levels of WNT/ β -catenin signaling and proliferation in the outer cortex. Ectopic expression of *Rspo1* by steroidogenic cells leads to increased WNT/ β -catenin signaling in the inner cortex, as indicated by ectopic expression of *Wnt4* and *Axin2*, and ectopic proliferation that causes adrenocortical hyperplasia and fragmentation of the medulla (M). On the contrary, in male adrenals or in female adrenals treated with androgens (DHT), ectopic *Rspo1* causes differential effects on *Wnt4* and *Axin2* expression, whereas ectopic proliferation is prevented via activation of AR signaling.

$\log_{10}(\text{FPKM}+1)$ expression values from differentially expressed genes as templates. Enriched gene sets were calculated using the Molecular Signatures database with an FDR q-value threshold of 0.05. GSEA (Subramanian et al., 2005) was conducted after DESeq2 was used via the GenePattern platform (Reich et al., 2006) to calculate differentially expressed genes between male and female GOF adrenals.

Statistical analysis

Statistical analysis was conducted as indicated in each figure legend using the GraphPad Prism 7 software. Given the complex nature of our genetic models, the number of samples were limited, and the sample size (n) reflects the number of animals available for each genotype.

Acknowledgements

We thank the staff of the animal facility for their help with animal husbandry and genotyping. We also thank Samah Rekima (histology platform) for help in analyzing RNA Scope quantification. We are grateful to S. Sacco, V. Vidal and R. Bandiera for initial analysis of the *Rspo1*^{GOF} phenotype, to D. Breault (Harvard University, USA) for the *AS-cre*, K. Parker for the *Sfl1-Cre* and *Ar* and J. Hilkins for the *Rspo3*^{GOF} alleles.

Competing interests

The authors declare no competing or financial interests.

Author contributions

Conceptualization: R.L., A.G., M.-C.C., A.S.; Methodology: R.L., A.G., A.S.; Validation: R.L., A.G., A.S.; Investigation: R.L., A.G., A.T., L.C.W.A., M.P., N.B., S.A.Y., A.d.B.; Resources: E.R.M.B., F.C., A.S.; Writing - original draft: R.L., A.S.; Writing - review & editing: R.L., A.G., A.T., M.P., N.B., S.A.Y., A.d.B., E.R.M.B., F.C., M.-C.C., A.S.; Visualization: R.L.; Supervision: R.L., M.-C.C., A.S.; Project administration: A.S.; Funding acquisition: R.L., N.B., A.d.B., A.S.

Funding

This work was funded by the Ligue Contre le Cancer (Equipe Labellisée 2018 to A.S.), the Agence Nationale de la Recherche (ANR-11-LABX-0028-01 and ANR-18-CE14-0012 to A.S.), Worldwide Cancer Research (WWCR 18-0437 to A.S.), the Fondation pour la Recherche Médicale (FRM SPF201809007141 to R.L.) and the Deutsche Forschungsgemeinschaft (CRC/Transregio 205/1, project no. 314061271, to A.S., M.P. and N.B.). Open Access funding provided by Université Côte d'Azur. Deposited in PMC for immediate release.

Data availability

RNA-seq data can be accessed at NCBI's Gene Expression Omnibus with the accession number GSE178958. All other data are available in the main text or the supplementary information.

First Person

This article has an associated First Person interview with the first author of the paper.

References

- Assié, G., Letouze, E., Fassnacht, M., Jouinot, A., Luscap, W., Barreau, O., Omeiri, H., Rodriguez, S., Perlemonne, K., René-Corail, F. et al. (2014). Integrated genomic characterization of adrenocortical carcinoma. *Nat. Genet.* **46**, 607-612. doi:10.1038/ng.2953
- Ayala-Ramirez, M., Jasim, S., Feng, L., Ejaz, S., Deniz, F., Busaidy, N., Waguespack, S. G., Naing, A., Sircar, K., Wood, C. G. et al. (2013). Adrenocortical carcinoma: clinical outcomes and prognosis of 330 patients at a tertiary care Center. *Eur. J. Endocrinol.* **169**, 891-899. doi:10.1530/EJE-13-0519
- Barrett, T., Wilhite, S. E., Ledoux, P., Evangelista, C., Kim, I. F., Tomashevsky, M., Marshall, K. A., Phillippy, K. H., Sherman, P. M., Holko, M. et al. (2013). NCBI GEO: archive for functional genomics data sets - Update. *Nucleic Acids Res.* **41**, D991-D995. doi:10.1093/nar/gks1193
- Basham, K. J., Rodriguez, S., Turcu, A. F., Lerario, A. M., Logan, C. Y., Rysztak, M. R., Gomez-Sanchez, C. E., Breault, D. T., Koo, B.-K., Clevers, H. et al. (2019). A ZNRF3-dependent Wnt/ β -catenin signaling gradient is required for adrenal homeostasis. *Genes Dev.* **33**, 209-220. doi:10.1101/gad.317412.118
- Berthon, A., Sahut-Barnola, I., Lambert-Langlais, S., de Jousineau, C., Damon-Soubeyrand, C., Louiset, E., Taketo, M. M., Tissier, F., Bertherat, J., Lefrançois-Martinez, A.-M. et al. (2010). Constitutive β -catenin activation induces adrenal hyperplasia and promotes adrenal cancer development. *Hum. Mol. Genet.* **19**, 1561-1576. doi:10.1093/hmg/ddq029
- Bielohuby, M., Herbach, N., Wanke, R., Maser-Gluth, C., Beuschlein, F., Wolf, E. and Hoeflich, A. (2007). Growth analysis of the mouse adrenal gland from weaning to adulthood: time- and gender-dependent alterations of cell size and number in the cortical compartment. *Am. J. Physiol. Metab.* **293**, E139-E146. doi:10.1152/ajpendo.00705.2006
- Bingham, N. C., Verma-Kurvari, S., Parada, L. F. and Parker, K. L. (2006). Development of a steroidogenic factor 1/Cre transgenic mouse line. *Genesis* **44**, 419-424. doi:10.1002/dvg.20231
- Borges, K. S., Pignatti, E., Leng, S., Kariyawasam, D., Ruiz-Babot, G., Ramalho, F. S., Taketo, M. M., Carlone, D. L. and Breault, D. T. (2020). Wnt/ β -catenin activation cooperates with loss of p53 to cause adrenocortical carcinoma in mice. *Oncogene* **39**, 5282-5291. doi:10.1038/s41388-020-1358-5
- Chang, S. P., Morrison, H. D., Nilsson, F., Kenyon, C. J., West, J. D. and Morley, S. D. (2013). Cell proliferation, movement and differentiation during maintenance of the adult mouse adrenal cortex. *PLoS One* **8**, e81865. doi:10.1371/journal.pone.0081865
- Chatterjee, P., Schweizer, M. T., Lucas, J. M., Coleman, I., Nyquist, M. D., Frank, S. B., Tharakan, R., Mostaghel, E., Luo, J., Pritchard, C. C. et al. (2019). Supraphysiological androgens suppress prostate cancer growth through androgen receptor-mediated DNA damage. *J. Clin. Invest.* **129**, 4245-4260. doi:10.1172/JCI127613
- Chen, X., McCluskey, R., Chen, J., Beaven, S. W. and Tontonoz, P. (2012). The number of X chromosomes causes sex differences in adiposity in mice. *PLoS Genet.* **8**, 1002709. doi:10.1371/journal.pgen.1002709
- Ching, S. and Vilain, E. (2009). Targeted disruption of Sonic Hedgehog in the mouse adrenal leads to adrenocortical hypoplasia. *Genesis* **47**, 628-637. doi:10.1002/dvg.20532
- Chistiakov, D. A., Killingsworth, M. C., Myasoedova, V. A., Orekhov, A. N. and Bobryshev, Y. V. (2017). CD68/macrosialin: not just a histochemical marker. *Lab. Invest.* **97**, 4-13. doi:10.1038/labinvest.2016.116
- Clocchiatti, A., Cora, E., Zhang, Y. and Dotto, G. P. (2016). Sexual dimorphism in cancer. *Nat. Rev. Cancer* **16**, 330-339. doi:10.1038/nrc.2016.30
- Crona, J. and Beuschlein, F. (2019). Adrenocortical carcinoma — towards genomics guided clinical care. *Nat. Rev. Endocrinol.* **15**, 548-560. doi:10.1038/s41574-019-0221-7
- Dai, C., Heemers, H. and Sharifi, N. (2017). Androgen signaling in prostate cancer. *Cold Spring Harb. Perspect. Med.* **7**, a030452. doi:10.1101/cshperspect.a030452
- De Cian, M.-C., Pauper, E., Bandiera, R., Vidal, V. P. I., Sacco, S., Gregoire, E. P., Chassot, A.-A., Panzolini, C., Wilhelm, D., Pailhoux, E. et al. (2017). Amplification of R-spondin1 signaling induces granulosa cell fate defects and cancers in mouse adult ovary. *Oncogene* **36**, 208-218. doi:10.1038/onc.2016.191
- De Gendt, K., Swinnen, J. V., Saunders, P. T. K., Schoonjans, L., Dewerchin, M., Devos, A., Tan, K., Atanassova, N., Claessens, F., Lécreuil, C. et al. (2004). A Sertoli cell-selective knockout of the androgen receptor causes spermatogenic arrest in meiosis. *Proc. Natl. Acad. Sci. USA* **101**, 1327-1332. doi:10.1073/pnas.0308114100
- Dolfi, B., Gallerand, A., Firulyova, M. M., Xu, Y., Merlin, J., Dumont, A., Castiglione, A., Vaillant, N., Quemener, S., Gerke, H. et al. (2022). Unravelling the sex-specific diversity and functions of adrenal gland macrophages. *Cell Rep.* **39**, 110949. doi:10.1016/j.celrep.2022.110949
- Dumont, T., Sahut-Barnola, I., Septier, A., Montanier, N., Plotton, I., Roucher-Boulez, F., Ducros, V., Lefrançois-Martinez, A.-M., Pointud, J.-C., Zubair, M. et al. (2018). PKA signaling drives reticularis differentiation and sexually dimorphic adrenal cortex renewal. *JCI Insight* **3**, e98394. doi:10.1172/jci.insight.98394
- El Wakil, A., Mari, B., Barhanin, J. and Lalli, E. (2013). Genomic analysis of sexual dimorphism of gene expression in the mouse adrenal gland. *Horm. Metab. Res.* **45**, 870-873. doi:10.1055/s-0033-1349881
- Fevr, T., Robine, S., Louvard, D. and Huelsen, J. (2007). Wnt/ β -catenin is essential for intestinal homeostasis and maintenance of intestinal stem cells. *Mol. Cell. Biol.* **27**, 7551-7559. doi:10.1128/MCB.01034-07
- Finco, I., Lerario, A. M. and Hammer, G. D. (2018). Sonic hedgehog and WNT signaling promote adrenal gland regeneration in male mice. *Endocrinology* **159**, 579-596. doi:10.1210/en.2017-03061
- Fischer, M. and Müller, G. A. (2017). Cell cycle transcription control: DREAM/MuvB and RB-E2F complexes. *Crit. Rev. Biochem. Mol. Biol.* **52**, 638-662. doi:10.1080/10409238.2017.1360836
- Fischer, M., Grossmann, P., Padi, M. and DeCaprio, J. A. (2016). Integration of TP53, DREAM, MMB-FOXM1 and RB-E2F target gene analyses identifies cell cycle gene regulatory networks. *Nucleic Acids Res.* **44**, 6070-6086. doi:10.1093/nar/gkw523
- Freedman, B. D., Kempna, P. B., Carlone, D. L., Shah, M., Guagliardo, N. A., Barrett, P. Q., Gomez-Sanchez, C. E., Majzoub, J. A. and Breault, D. T. (2013). Adrenocortical zonation results from lineage conversion of differentiated zona glomerulosa cells. *Dev. Cell* **26**, 666-673. doi:10.1016/j.devcel.2013.07.016
- Gannon, A.-L., O'Hara, L., Mason, J. I., Jørgensen, A., Frederiksen, H., Milne, L., Smith, S., Mitchell, R. T. and Smith, L. B. (2019). Androgen receptor signalling in the male adrenal facilitates X-zone regression, cell turnover and protects against adrenal degeneration during ageing. *Sci. Rep.* **9**, 10457. doi:10.1038/s41598-019-46049-3
- Gao, S., Gao, Y., Hansen, H., Chen, S., Balk, S. P. and Cai, C. (2016). Androgen receptor tumor suppressor function is mediated by recruitment of retinoblastoma

- protein accession numbers GSE76141. *Cell Rep.* **17**, 966-976. doi:10.1016/j.celrep.2016.09.064
- Goel, N., Workman, J. L., Lee, T. T., Innala, L. and Viau, V. (2014). Sex differences in the HPA axis. *Compr. Physiol.*, **4**, 1121-1155. doi:10.1002/cphy.c130054
- Grabek, A., Dolfi, B., Klein, B., Jian-Motamedi, F., Chaboissier, M.-C. and Schedl, A. (2019). The adult adrenal cortex undergoes rapid tissue renewal in a sex-specific manner. *Cell Stem Cell* **25**, 290-296.e2. doi:10.1016/j.stem.2019.04.012
- Hao, H. X., Xie, Y., Zhang, Y., Zhang, O., Oster, E., Avello, M., Lei, H., Mickanin, C., Liu, D., Ruffner, H. et al. (2012). ZNRF3 promotes Wnt receptor turnover in an R-spondin-sensitive manner. *Nature* **485**, 195-202. doi:10.1038/nature11019
- Heikkilä, M., Peltoketo, H., Leppäluoto, J., Ilves, M., Vuolteenaho, O. and Vainio, S. (2002). Wnt-4 deficiency alters mouse adrenal cortex function, reducing aldosterone production. *Endocrinology* **143**, 4358-4365. doi:10.1210/en.2002-220275
- Hickey, T. E., Selth, L. A., Chia, K. M., Laven-Law, G., Milioli, H. H., Roden, D., Jindal, S., Hui, M., Finlay-Schultz, J., Ebrahimie, E. et al. (2021). The androgen receptor is a tumor suppressor in estrogen receptor-positive breast cancer. *Nat. Med.* **27**, 310-320. doi:10.1038/s41591-020-01168-7
- Hilkens, J., Timmer, N. C., Boer, M., Ikink, G. J., Schewe, M., Sacchetti, A., Koppens, M. A. J., Song, J.-Y. and Bakker, E. R. M. (2017). RSPO3 expands intestinal stem cell and niche compartments and drives tumorigenesis. *Gut* **66**, 1095-1105. doi:10.1136/gutjnl-2016-311606
- Huang, C.-C. J. and Kang, Y. (2019). The transient cortical zone in the adrenal gland: the mystery of the adrenal X-zone. *J. Endocrinol.* **241**, R51-R63. doi:10.1530/JOE-18-0632
- Ishii, T., Mitsui, T., Suzuki, S., Matsuzaki, Y. and Hasegawa, T. (2012). A genome-wide expression profile of adrenocortical cells in knockout mice lacking steroidogenic acute regulatory protein. *Endocrinology* **153**, 2714-2723. doi:10.1210/en.2011-1627
- Jho, E., Zhang, T., Domon, C., Joo, C.-K., Freund, J.-N. and Costantini, F. (2002). Wnt/ β -Catenin/Tcf signaling induces the transcription of Axin2, a negative regulator of the signaling pathway. *Mol. Cell. Biol.* **22**, 1172-1183. doi:10.1128/MCB.22.4.1172-1183.2002
- Karp, N. A., Mason, J., Beaudet, A. L., Benjamini, Y., Bower, L., Braun, R. E., Brown, S. D. M., Chesler, E. J., Dickinson, M. E., Flenniken, A. M. et al. (2017). Prevalence of sexual dimorphism in mammalian phenotypic traits. *Nat. Commun.* **8**, 15475. doi:10.1038/ncomms15475
- Kim, A. C., Reuter, A. L., Zubair, M., Else, T., Serecky, K., Bingham, N. C., Lavery, G. G., Parker, K. L. and Hammer, G. D. (2008). Targeted disruption of β -catenin in Sf1-expressing cells impairs development and maintenance of the adrenal cortex. *Development* **135**, 2593-2602. doi:10.1242/dev.021493
- King, P., Paul, A. and Lauffer, E. (2009). Shh signaling regulates adrenocortical development and identifies progenitors of steroidogenic lineages. *Proc. Natl. Acad. Sci. USA* **106**, 21185-21190. doi:10.1073/pnas.0909471106
- Klein, S. L. and Flanagan, K. L. (2016). Sex differences in immune responses. *Nat. Rev. Immunol.* **16**, 626-638. doi:10.1038/nri.2016.90
- Kleverov, M., Zenkova, D., Kamenev, V., Sablina, M., Artyomov, M. N. and Sergushichev, A. A. (2022). Phantassus: web-application for visual and interactive gene expression analysis. *bioRxiv* 2022.12.10.519861.
- Kretzschmar, K., Cottle, D. L., Schweiger, P. J. and Watt, F. M. (2015). The androgen receptor antagonizes Wnt/ β -Catenin signaling in epidermal stem cells. *J. Invest. Dermatol.* **135**, 2753-2763. doi:10.1038/jid.2015.242
- Lacroix, A., Feelders, R. A., Stratakis, C. A. and Nieman, L. K. (2015). Cushing's syndrome. *Lancet* **386**, 913-927. doi:10.1016/S0140-6736(14)61375-1
- Leng, S., Pignatti, E., Khetani, R. S., Shah, M. S., Xu, S., Miao, J., Taketo, M. M., Beuschlein, F., Barrett, P. Q., Carlone, D. L. et al. (2020). β -Catenin and FGFR2 regulate postnatal rosette-based adrenocortical morphogenesis. *Nat. Commun.* **11**, 1680. doi:10.1038/s41467-020-15332-7
- Lindholm, J., Juul, S., Jørgensen, J. O. L., Astrup, J., Bjerre, P., Feldt-Rasmussen, U., Hagen, C., Jørgensen, J., Kosteljanetz, M., Kristensen, L. Ø. et al. (2001). Incidence and late prognosis of Cushing's syndrome: a population-based study 1. *J. Clin. Endocrinol. Metab.* **86**, 117-123. doi:10.1210/jcem.86.1.7093
- Litvinov, I. V., Vander Griend, D. J., Antony, L., Dalrymple, S., De Marzo, A. M., Drake, C. G. and Isaacs, J. T. (2006). Androgen receptor as a licensing factor for DNA replication in androgen-sensitive prostate cancer cells. *Proc. Natl. Acad. Sci. USA* **103**, 15085-15090. doi:10.1073/pnas.0603057103
- Luton, J. P., Cerdas, S., Billaud, L., Thomas, G., Guilhaume, B., Bertagna, X., Laudat, M. H., Louvel, A., Chapuis, Y., Blondeau, P. et al. (1990). Clinical features of adrenocortical carcinoma, prognostic factors, and the effect of mitotane therapy. *N. Engl. J. Med.* **322**, 1195-1201. doi:10.1056/NEJM199004263221705
- Lyraki, R. and Schedl, A. (2021a). The sexually dimorphic adrenal cortex: implications for adrenal disease. *Int. J. Mol. Sci.* **22**, 4889. doi:10.3390/ijms22094889
- Lyraki, R. and Schedl, A. (2021b). Adrenal cortex renewal in health and disease. *Nat. Rev. Endocrinol.* **17**, 421-434. doi:10.1038/s41574-021-00491-4
- Mulholland, D. J., Read, J. T., Rennie, P. S., Cox, M. E. and Nelson, C. C. (2003). Functional localization and competition between the androgen receptor and T-cell factor for nuclear β -catenin: a means for inhibition of the Tcf signaling axis. *Oncogene* **22**, 5602-5613. doi:10.1038/sj.onc.1206802
- Muto, S., Enta, A., Maruya, Y., Inomata, S., Yamaguchi, H., Mine, H., Takagi, H., Ozaki, Y., Watanabe, M., Inoue, T. et al. (2023). Wnt/ β -catenin signaling and resistance to immune checkpoint inhibitors: from non-small-cell lung cancer to other cancers. *Biomedicines* **11**, 190. doi:10.3390/biomedicines11010190
- Nusse, R. and Clevers, H. (2017). Wnt/ β -catenin signaling, disease, and emerging therapeutic modalities. *Cell* **169**, 985-999. doi:10.1016/j.cell.2017.05.016
- Peitzsch, M., Dekkers, T., Haase, M., Sweep, F. C. G. J., Quack, I., Antoch, G., Siebert, G., Lenders, J. W. M., Deinum, J., Willenberg, H. S. et al. (2015). An LC-MS/MS method for steroid profiling during adrenal venous sampling for investigation of primary aldosteronism. *J. Steroid Biochem. Mol. Biol.* **145**, 75-84. doi:10.1016/j.jsbmb.2014.10.006
- Pignatti, E., Leng, S., Carlone, D. L. and Breault, D. T. (2017). Regulation of zonation and homeostasis in the adrenal cortex. *Mol. Cell. Endocrinol.* **441**, 146-155. doi:10.1016/j.mce.2016.09.003
- Pignatti, E., Leng, S., Yuchi, Y., Borges, K. S., Guagliardo, N. A., Shah, M. S., Ruiz-Babot, G., Kariyawasam, D., Taketo, M. M., Miao, J. et al. (2020). Beta-catenin causes adrenal hyperplasia by blocking zonal transdifferentiation. *Cell Rep.* **31**, 107524. doi:10.1016/j.celrep.2020.107524
- Reich, M., Liefeld, T., Gould, J., Lerner, J., Tamayo, P. and Mesirov, J. P. (2006). GenePattern 2.0 [2]. *Nat. Genet.* **38**, 500-501. doi:10.1038/ng0506-500
- Rocha, A. S., Vidal, V., Mertz, M., Kendall, T. J., Charlet, A., Okamoto, H. and Schedl, A. (2015). The angiocrine factor Rspondin3 is a key determinant of liver zonation. *Cell Rep.* **13**, 1757-1764. doi:10.1016/j.celrep.2015.10.049
- Rossi, R., Zatelli, M. C., Valentini, A., Cavazzini, P., Fallo, F., Del Senno, L. and Uberti, E. C. D. (1998). Evidence for androgen receptor gene expression and growth inhibitory effect of dihydrotestosterone on human adrenocortical cells. *J. Endocrinol.* **159**, 373-380. doi:10.1677/joe.0.1590373
- Sahut-Barnola, I., Lefrançois-Martinez, A. M., Jean, C., Veysiere, G. and Martinez, A. (2000). Adrenal tumorigenesis targeted by the corticotropin-regulated promoter of the Aldo-Keto reductase AKR1B7 gene in transgenic mice. *Endocr. Res.* **26**, 885-898. doi:10.3109/07435800009048613
- Sansom, O. J., Meniel, V. S., Muncan, V., Phesse, T. J., Wilkins, J. A., Reed, K. R., Vass, J. K., Athineos, D., Clevers, H. and Clarke, A. R. (2007). Myc deletion rescues Apc deficiency in the small intestine. *Nature* **446**, 676-679. doi:10.1038/nature05674
- Scollo, C., Russo, M., Trovato, M. A., Sambataro, D., Giuffrida, D., Manusia, M., Sapuppo, G., Malandrino, P., Vigneri, R. and Pellegriti, G. (2016). Prognostic factors for adrenocortical carcinoma outcomes. *Front. Endocrinol.* **7**, 99. doi:10.3389/fendo.2016.00099
- Seale, J. V., Wood, S. A., Atkinson, H. C., Harbuz, M. S. and Lightman, S. L. (2004). Gonadal steroid replacement reverses gonadectomy-induced changes in the corticosterone pulse profile and stress-induced hypothalamic-pituitary-adrenal axis activity of male and female rats. *J. Neuroendocrinol.* **16**, 989-998. doi:10.1111/j.1365-2826.2004.01258.x
- Shtutman, M., Zhurinsky, J., Simcha, I., Albanese, C., D'Amico, M., Pestell, R. and Ben-Ze'ev, A. (1999). The cyclin D1 gene is a target of the beta-catenin/LEF-1 pathway. *Proc. Natl. Acad. Sci. USA* **96**, 5522-5527. doi:10.1073/pnas.96.10.5522
- Subramanian, A., Tamayo, P., Mootha, V. K., Mukherjee, S., Ebert, B. L., Gillette, M. A., Paulovich, A., Pomeroy, S. L., Golub, T. R., Lander, E. S. et al. (2005). Gene set enrichment analysis: a knowledge-based approach for interpreting genome-wide expression profiles. *Proc. Natl. Acad. Sci. USA* **102**, 1545-1550. doi:10.1073/pnas.0506580102
- Van de Wetering, M., Sancho, E., Verweij, C., De Lau, W., Oving, I., Hurlstone, A., Van der Horn, K., Batlle, E., Coudreuse, D., Haramis, A. P. et al. (2002). The β -catenin/TCF-4 complex imposes a crypt progenitor phenotype on colorectal cancer cells. *Cell* **111**, 241-250. doi:10.1016/S0092-8674(02)01014-0
- Vidal, V. P. I., Chaboissier, M.-C., de Rooij, D. G. and Schedl, A. (2001). Sox9 induces testis development in XX transgenic mice. *Nat. Genet.* **28**, 216-217. doi:10.1038/90046
- Vidal, V., Sacco, S., Rocha, A. S., da Silva, F., Panzolini, C., Dumontet, T., Doan, T. M. P., Shan, J., Rak-Raszewska, A., Bird, T. et al. (2016). The adrenal capsule is a signaling center controlling cell renewal and zonation through Rspo3. *Genes Dev.* **30**, 1389-1394. doi:10.1101/gad.277756.116
- Wilmouth, J. J., Olabe, J., Garcia-Garcia, D., Lucas, C., Guiton, R., Roucher-Boulez, F., Dufour, D., Damon-Soubeyrand, C., Sahut-Barnola, I., Pointud, J. C. et al. (2022). Sexually dimorphic activation of innate antitumor immunity prevents adrenocortical carcinoma development. *Sci. Adv.* **8**, eadd0422. doi:10.1126/sciadv.add0422
- Xie, X., Lu, J., Kulbokas, E. J., Golub, T. R., Mootha, V., Lindblad-Toh, K., Lander, E. S. and Kellis, M. (2005). Systematic discovery of regulatory motifs in human promoters and 3' UTRs by comparison of several mammals. *Nature* **434**, 338-345. doi:10.1038/nature03441
- Yu, X., Li, S., Xu, Y., Zhang, Y., Ma, W., Liang, C., Lu, H., Ji, Y., Liu, C., Chen, D. et al. (2020). Androgen maintains intestinal homeostasis by inhibiting BMP signaling via intestinal stromal cells. *Stem Cell Reports* **15**, 912-925. doi:10.1016/j.stemcr.2020.08.001

Zebisch, M., Xu, Y., Krastev, C., Macdonald, B. T., Chen, M., Gilbert, R. J. C., He, X. and Jones, E. Y. (2013). Structural and molecular basis of ZNRF3/RNF43 transmembrane ubiquitin ligase inhibition by the Wnt agonist R-spondin. *Nat. Commun.* **4**, 2787. doi:10.1038/ncomms3787

Zheng, S., Cherniack, A. D., Dewal, N., Moffitt, R. A., Danilova, L., Murray, B. A., Lerario, A. M., Else, T., Krijnenburg, T. A., Ciriello, G. et al. (2016). Comprehensive pan-genomic characterization of adrenocortical carcinoma. *Cancer Cell* **29**, 723-736. doi:10.1016/j.ccell.2016.04.002

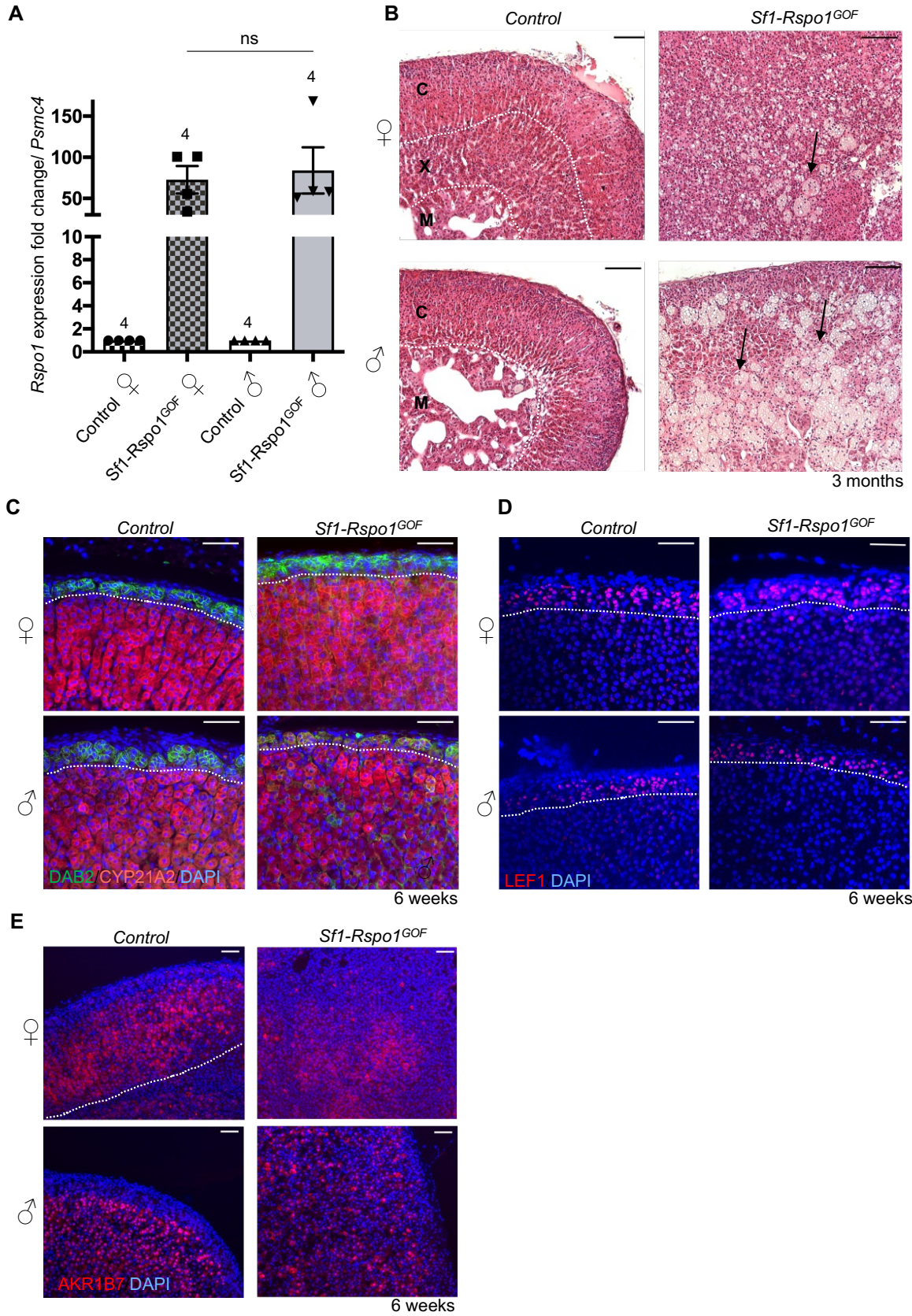


Fig. S1. Characterization of RSPO1 overexpression and its effects on adrenocortical cells.

A) RT-qPCR analysis of *Rspo1* expression relative to *Psmc4* in adrenals from 6-week-old mice, shown as mean fold change in *Sfl-Rspo1^{GOF}* adrenals compared to sex-matched controls. The numbers below the graph columns represent number of samples in each group (n). The numbers above the graph columns represent number of samples in each group (n=4). Statistical analysis was performed using unpaired two-tailed t-test (P=0.7442). Error bars represent the standard error of the mean (SEM). B) H&E staining of adrenal sections from 3-month-old mice. Black arrows point to the vacuolated cells forming degenerative lesions. C: cortex, X: x-zone, M: medulla. Scale bar: 100 μ m. C) Immunofluorescence staining for DAB2 (marker of the zG) and CYP21A2 (marker of adrenal steroidogenic cells), using adrenal sections from 6-week-old mice. Scale bar: 50 μ m. D) Immunofluorescence staining for LEF1 (marker of the zG) on adrenal sections from 6-week-old mice. Scale bar: 50 μ m. E) Immunofluorescence staining for the aldo-keto reductase AKR1B7 using adrenal sections from 6-week-old mice. Scale bar: 50 μ m.

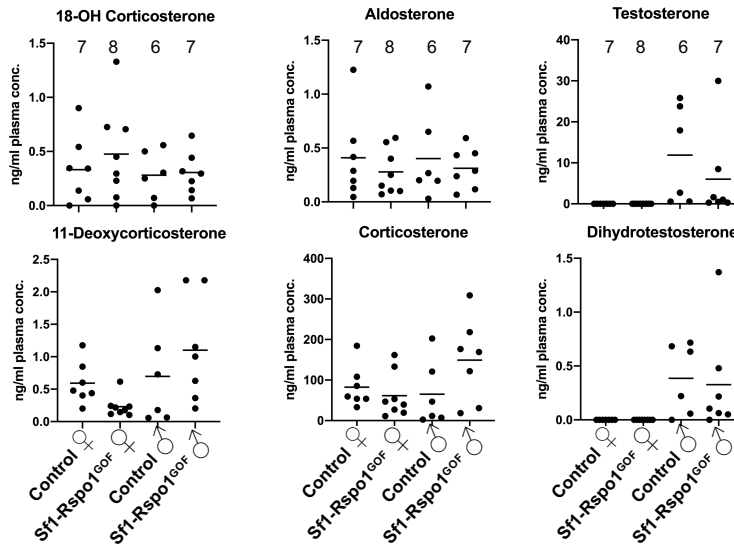


Fig. S2. Plasma steroid levels. Quantification of adrenal and testicular steroids in the plasma of control and *Sf1-Rspo1*^{GOF} mice at 6 weeks of age by liquid chromatography paired with tandem mass spectrometry (LC-MS/MS). The numbers above the graph columns represent number of samples in each group (n).

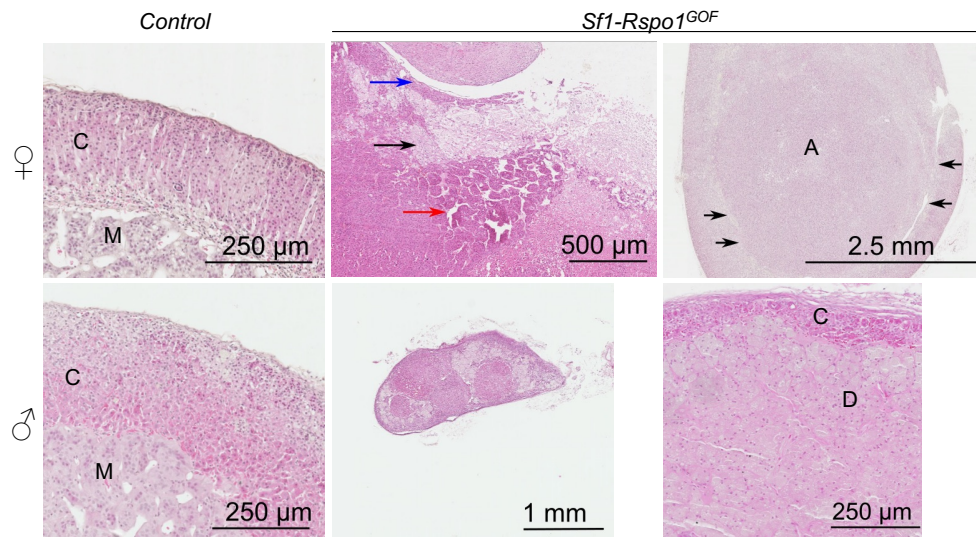


Fig. S3. Ectopic RSPO1 expression leads to the development of nodules and neoplasia in aging animals. On the top panel, representative H&E images of 12-month-old female control and *Sf1-Rspo1^{GOF}* adrenals are shown. Both female *Sf1-Rspo1^{GOF}* adrenals have tumors: in the middle, the adrenal is completely effaced by an adrenocortical carcinoma. Capsular invasion (blue arrow) and areas of extended necrosis (black arrow) and nest-like cell organization (red arrow) can be seen. On the left, the adrenal harbors a well-circumscribed adrenocortical adenoma. On the bottom panel, representative H&E staining on 12-month-old male control and *Sf1-Rspo1^{GOF}* adrenals shows the extensive degeneration and cortical thinning paired with incidences of nodular hyperplasia in the *Sf1-Rspo1^{GOF}* adrenals. C: cortex, M: medulla, D: degeneration, A: adenoma.

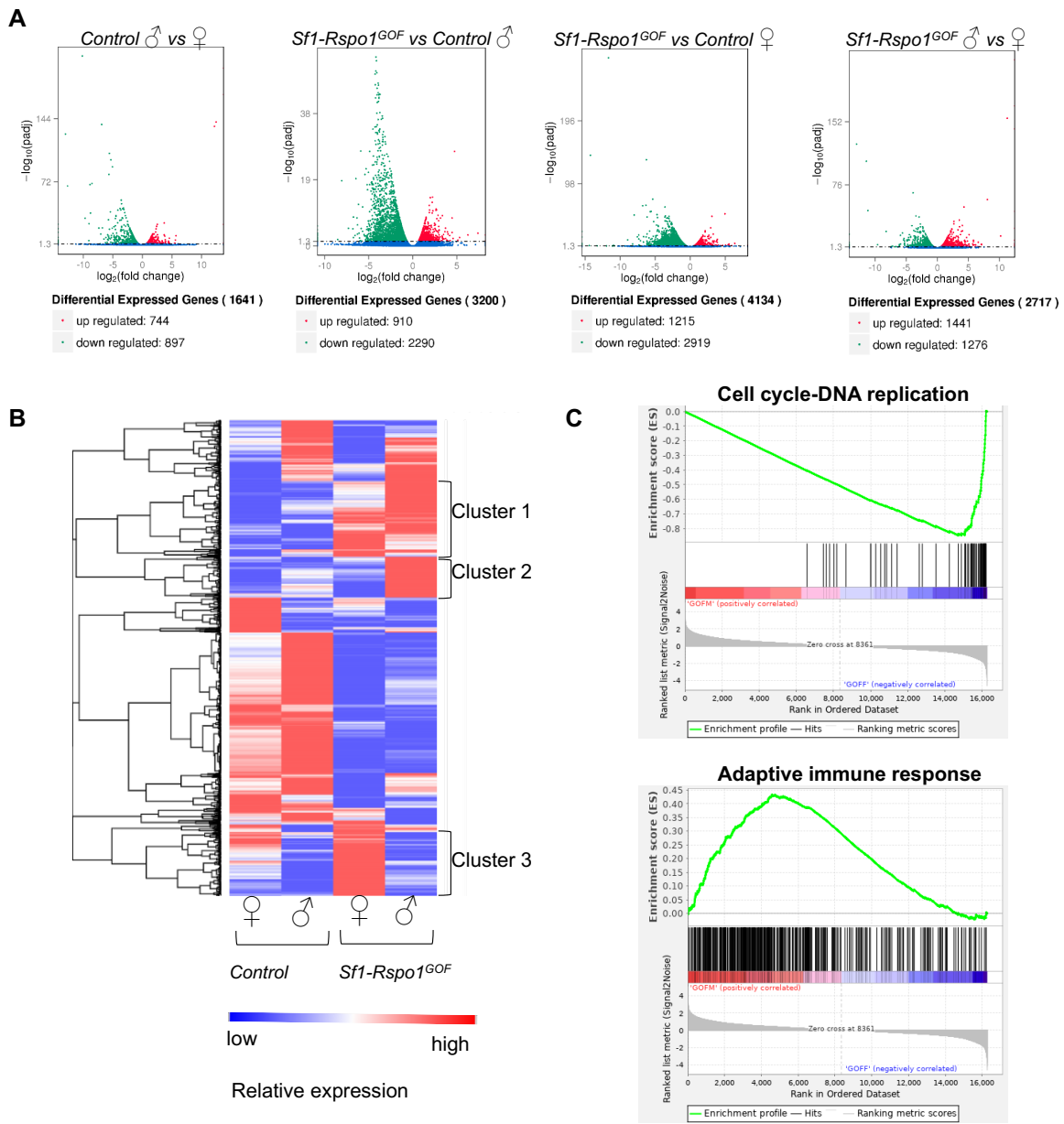


Fig. S4. Analysis of differential gene expression between groups. A) Volcano plots differentially expressed genes between pairs of experimental groups. B) Hierarchical clustering and heatmap representation of differential gene expression among control and *Sf1-Rspo1*^{GOF}, male and female adrenals. Relative expression differences are shown in color code. C) Enrichment plots for gene ontology (GO) terms produced by GSEA analysis comparing male ('GOFM') to female ('GOFF') *Sf1-Rspo1*^{GOF} adrenals.

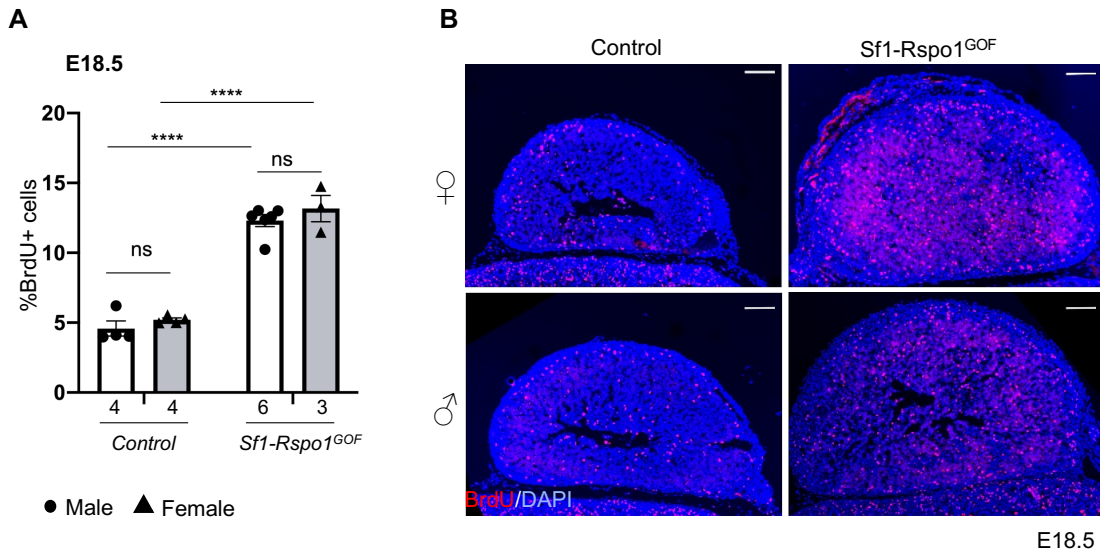


Fig. S5. Male and female $Rspo1^{GOF}$ embryos display equal rates of adrenocortical cell proliferation. A) BrdU proliferation analysis shown as mean percentage of proliferating cells over total number of cells in the adrenal cortex of E18.5 mouse embryos (error bars represent SEM). The numbers below the graph columns represent number of samples in each group (n). Statistical analysis was conducted using ordinary two-way ANOVA followed by Tukey's multiple comparison's test. Adjusted p-values: Control F vs $Sf1-Rspo1^{GOF}$ F: $P < 0.0001$, Control M vs $Sf1-Rspo1^{GOF}$ M: $P < 0.0001$, $Sf1-Rspo1^{GOF}$ F vs $Sf1-Rspo1^{GOF}$ M: $P = 0.6680$. B) Representative images of BrdU immunostaining in E18.5 adrenals. Scale bars: 100 μ m.

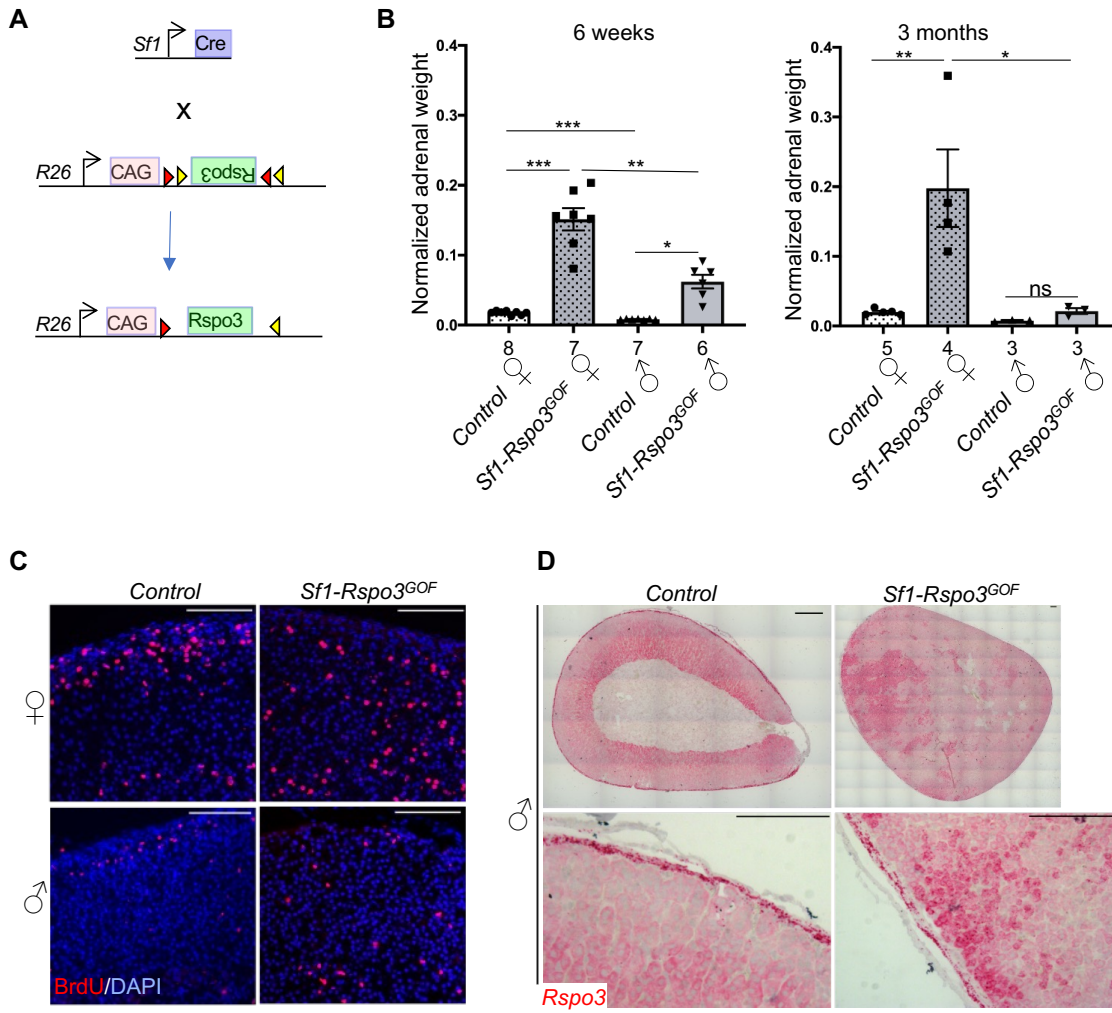


Fig. S6. Ectopic RSPO3 expression results in female-specific hyperplasia. A) Schematic representation of the genetic strategy to overexpress RSPO3 in adrenocortical cells using Sfl-Cre. B) Mean adrenal weight normalized to total body weight from 6 week and 3-month-old male and female control or *Sfl-Rspo3^{GOF}* adrenals. Error bars represent SEM. The numbers below the graph columns represent number of samples in each group (n). Statistical analysis for 6 weeks was conducted using Welch's one-way ANOVA followed by the Dunnett's T3 multiple comparisons test. Adjusted P-values: Control F vs *Sfl-Rspo3^{GOF}* F: P= 0.0008, Control F vs Control M: P=0.0001, *Sfl-Rspo3^{GOF}* F vs *Sfl-Rspo3^{GOF}* M: P=0.0043, Control M vs *Sfl-Rspo3^{GOF}* M: P=0.0130. Statistical analysis for 3 months was conducted with one-way standard ANOVA followed by Tukey's post-hoc test. Adjusted P-values: Control F vs *Sfl-Rspo3^{GOF}* F: P=0.0039, *Sfl-Rspo3^{GOF}* F vs *Sfl-Rspo3^{GOF}* M: P=0.0102, Control M vs *Sfl-Rspo3^{GOF}* M: P=0.9910. C) BrdU analysis to label proliferative cells in control and *Sfl-Rspo3^{GOF}* adrenal at 6 weeks of age. D) In situ hybridization for *Rspo3* using the RNA Scope method (*Rspo3* mRNA shown as red dots). Representative images represent control and *Sfl-Rspo3^{GOF}* adrenals from male 6-week-old animals. Scale bars: 50 μ m.

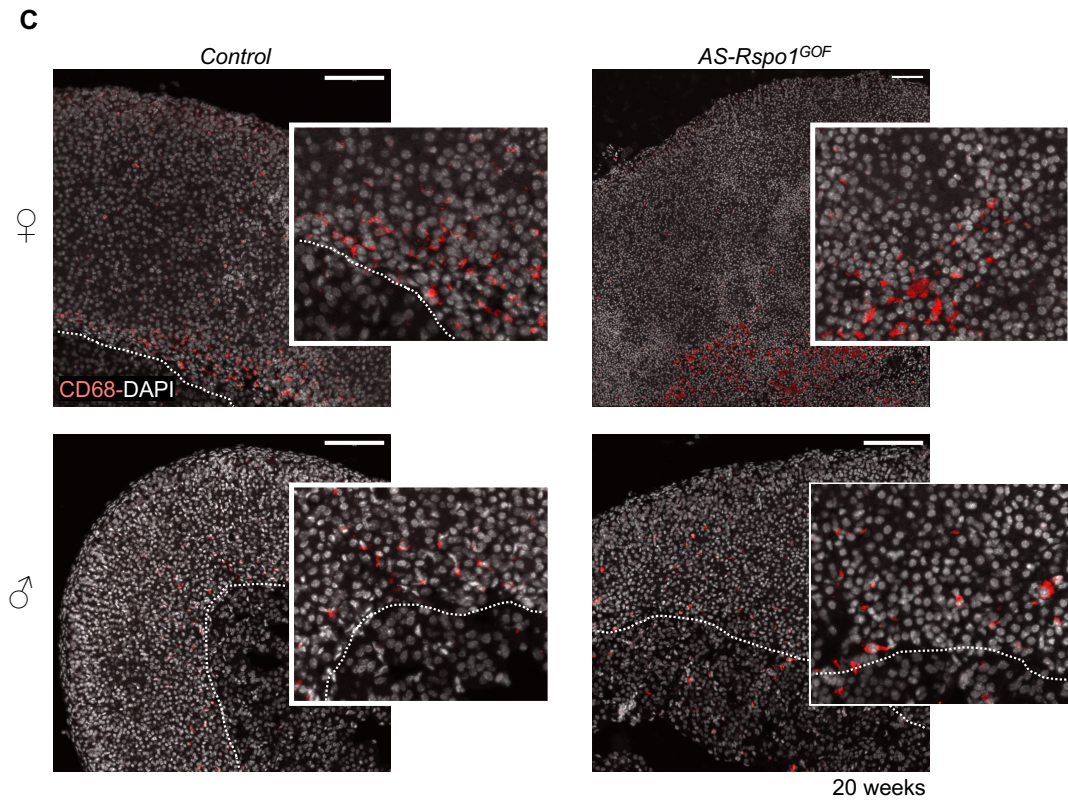
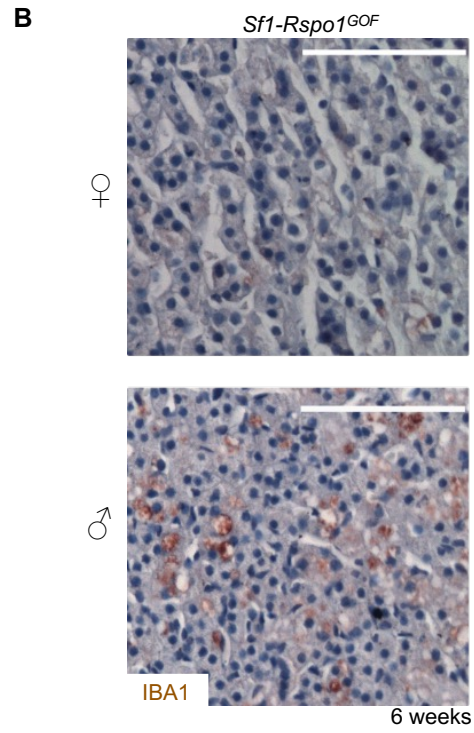
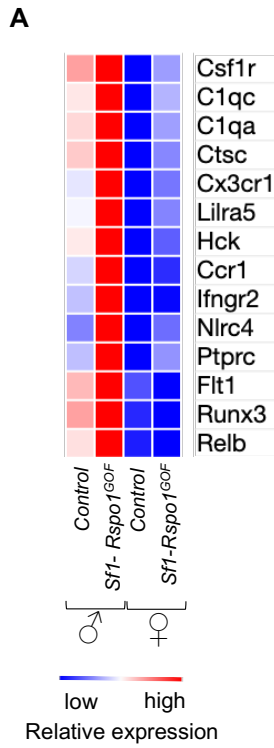
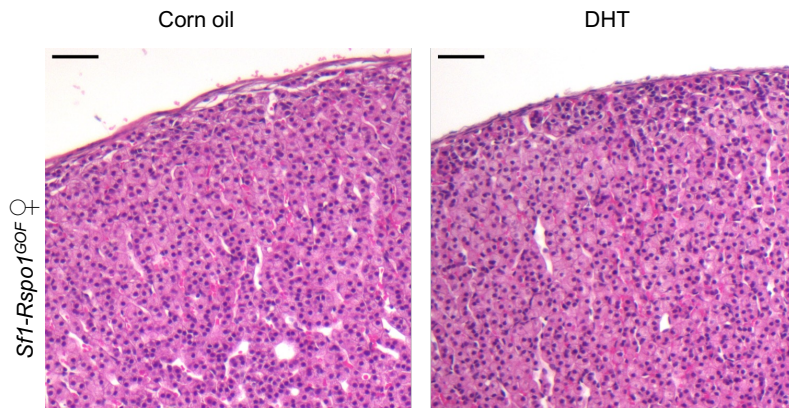
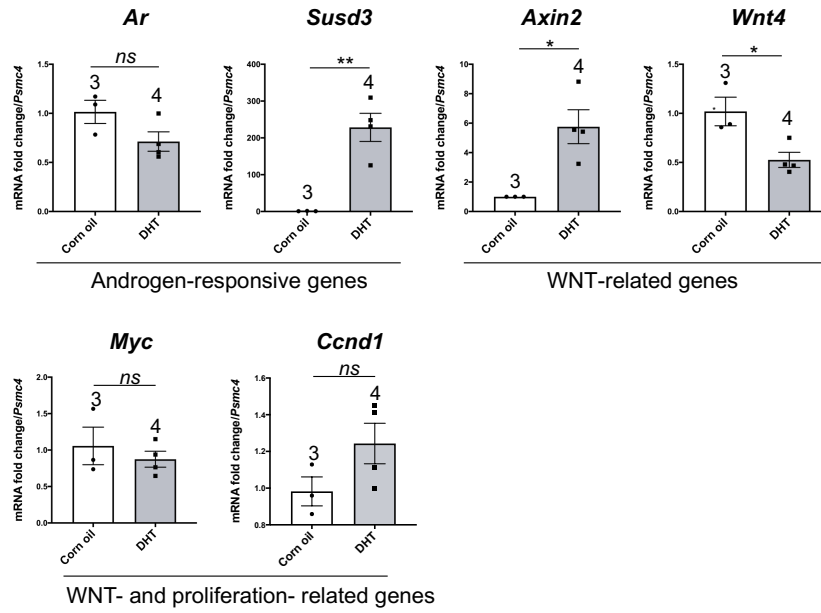


Fig. S7. Degenerative lesion formation by macrophages in the male *Sfl-Rspo1^{GOF}* adrenal cortex. A) Heatmap representation of relative expression differences (shown in color code) for genes expressed in macrophages/monocytes or pan-immune cells. B) Immunohistochemical staining for IBA1, a macrophage marker enriched in StAR deficient adrenals. Scale bar: 50 μm . C) Immunofluorescence staining for macrophage marker CD68 on 20-week-old adrenal cortex from control and *AS-Rspo1^{GOF}* animals. Scale bar: 100 μm .

A



B



C

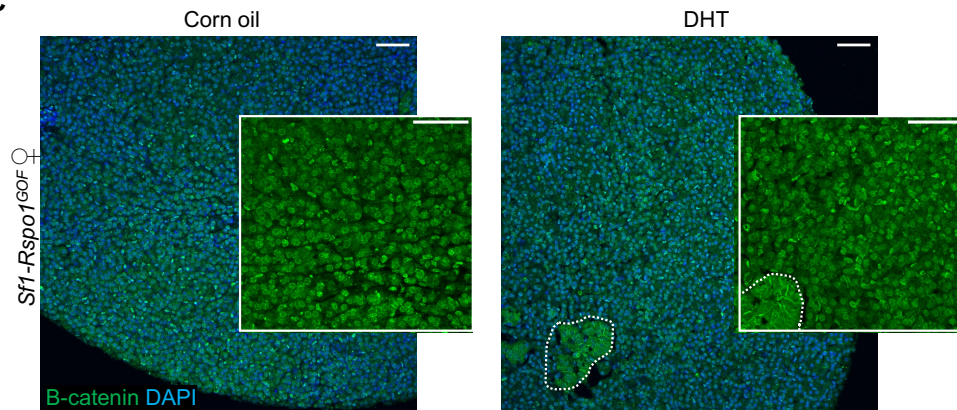


Fig. S8. Effect of DHT treatment on histology and expression in *Sfl-Rspo1^{GOF}* adrenals.

A) H&E staining on adrenal sections from 6-week-old female mice treated with corn oil or DHT during puberty. Scale bar: 50 μ m. B) RT-qPCR analysis of gene expression for WNT signaling target genes (*Wnt4*, *Axin2*), known target genes of WNT signaling also related to proliferation (*Myc*, *Ccnd1*), and genes possibly related to androgen receptor signaling (*Ar*, *Susd3*). Graphs represent mean fold expression change comparing corn oil to DHT treated adrenals (normalized to *Psmc4* expression). Error bars represent SEM. The numbers above the graph columns represent number of samples in each group (n). Statistical analysis was conducted with unpaired t-test. P values: 0.1056 (*Ar*), 0.0173 (*Axin2*), 0.0228 (*Wnt4*), 0.0040 (*Susd3*), 0.5019 (*Myc*), 0.1347 (*Ccnd1*). DHT: dihydrotestosterone. C) Immunofluorescence staining for β -catenin on adrenal sections from 6-week-old female mice treated with corn oil or DHT during puberty. Inserts represent zoomed-in areas of the inner cortex. Scale bar: 100 μ m

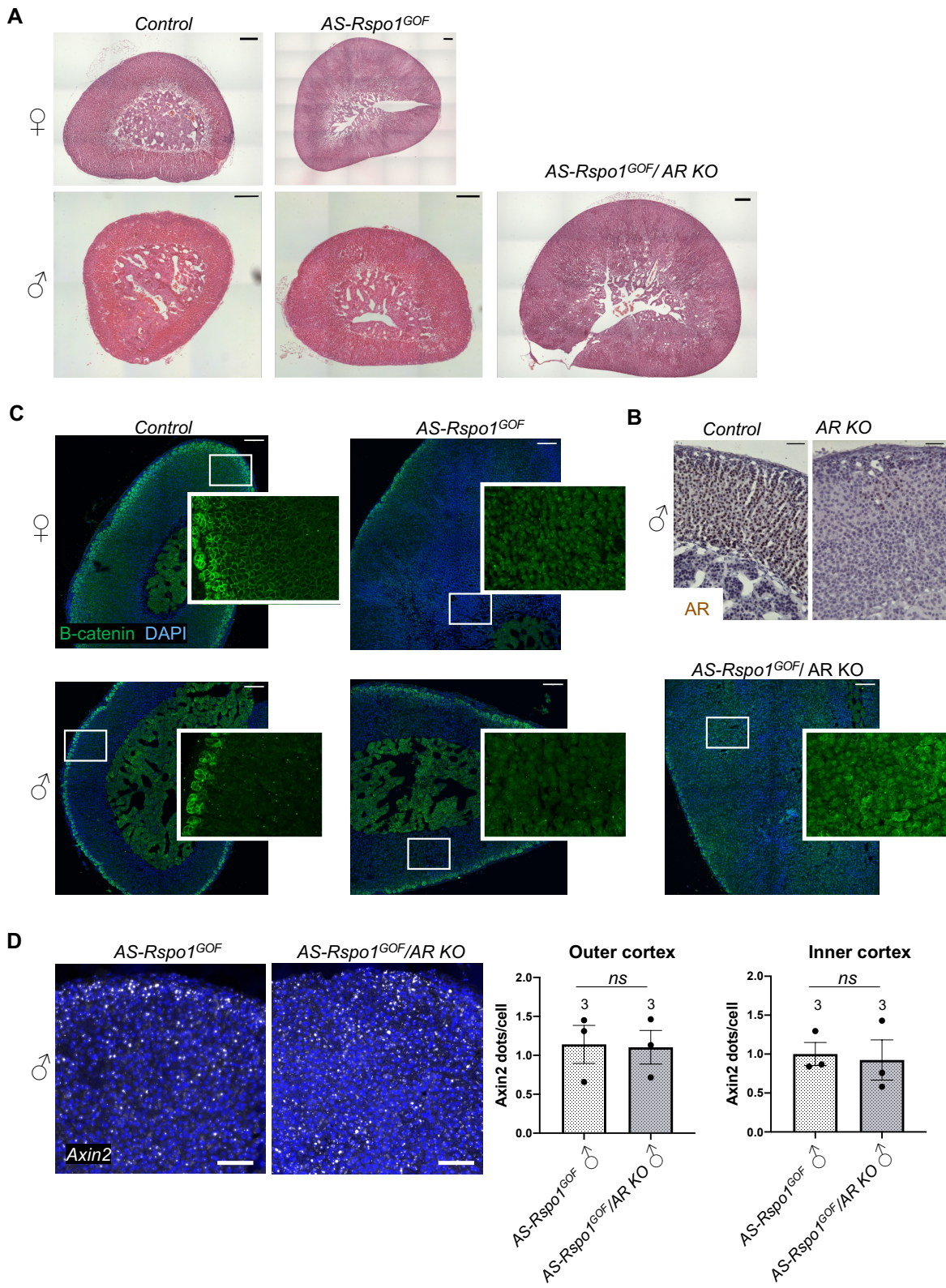


Fig. S9. Effect of *Ar* knock-out in adrenocortical histology, AR expression, and WNT signaling. A) Hematoxylin and eosin staining of adrenal sections at 20 weeks of age. Scale bar: 200 μm . B) Representative images of immunohistochemistry to detect AR in control and *Ar KO* male adrenals at 20 weeks of age. White arrows point to a few nuclei that display residual expression of AR in the *Ar KO* adrenals. Scale bar: 50 μm . C) Immunofluorescence staining for β -catenin on adrenal sections at 20 weeks of age. Inserts represent zoomed-in areas of the inner cortex. Scale bars: 100 μm . D) Quantification of *Axin2* expression on sections from *AS-Rspo1^{GOF}* and *AS-Rspo1^{GOF}/AR KO* male adrenals using RNA Scope single-molecule (ISH). The numbers above the graph columns represent number of samples in each group (n=3). Two-tailed unpaired t-test was used to determine statistical significance. Scale bars: 50 μm .

Table S1. List of primers used in this study.

Gene	Forward primer	Reverse primer 1	Reverse primer 2	Purpose
<i>Psmc4</i>	TTCTTGGAAGCTGTGG ATCA	TCAGGATGCGCACATAATA GTT		qPCR
<i>Rspo1</i>	CAGTGA CTATGCGGCT TGG	AGAGCTCACAGCCCTTGG		qPCR
<i>Susd3</i>	GACTGTGCTCATATTCC ACTGC	TAAAGCCGAAGGTCTCAT GC		qPCR
<i>Ar</i>	GTGCCACCCAAAGGA CT	CCTTTTCCCAATGCCTCAG CT		qPCR
<i>Pena</i>	CTAGCCATGGGCGTGA AC	GAATACTAGTGCTAAGGT GTCTGCAT		qPCR
<i>Pola1</i>	TGCACTGTGGATAAAT TCTCAAG	CAGTGAGGTTTGACCCAT CC		qPCR
<i>Cdc6</i>	TCCGTGTGTGGACGTA AAAC	GGAGTGTTGCACAGGTTG TC		qPCR
<i>E2f8</i>	CCAGAAATCAGCCCAA ACA	GCAGACTGCTCAGCCTCT AAG		qPCR
<i>Cnd1</i>	GCAGAAGGAGATTGTG CCATCC	AGGAAGCGGTCCAGGTAG TTCA		qPCR
<i>Myc</i>	CCTAGTGCTGCATGAG GA GA	TCCACAGACACCACATCA ATTT		qPCR
<i>Rspo1</i> transgene	TGTTCAITGTCGGGGTT GCGG	CGACCTGCAGCCCAAGCT AG		Genotyping
<i>Rosa26</i>	AGGGAGCTGCAGTGG AGTAG	AGCCTGCCCAGAAGACTC CC		Genotyping
Sfl1-Cre	CCCACCGTCAGTACGT GAGATATC	CGCGGTCTGGCAGTAAAA ACTAT		Genotyping
<i>Rspo3</i> transgene	CGGATTAATCGATCC CG	CCTATCTGCTTCATGCCAA TCC		Genotyping
<i>Wt1-Sox9</i> transgene	CATCCGAGCCGCACCT CATG	GCTGGAGCCGTTGACGCG		Genotyping
<i>Cyp11b2- Cre</i>	GAGCTGGGGCCCATTT TCAGG	GCTCCAGGTGCATCCGAC GG	AACTTGCACCAT GCCGCCA	Genotyping
<i>Sry</i>	TTGTCTAGAGAGCATG GAGGGCCATGTCAA	AACTTGCACCATGCCGCC CA		Genotyping
<i>Ar flox</i>	AGCCTGTATACTCAGTT GGGG	AATGCATCACATTAAGTTG ATACC		Genotyping

Table S2. List of antibodies used in this study.

Primary antibodies	Source	Reference	Dilution
Anti-Tyrosine hydroxylase (TH)	Sigma-Aldrich	AB152	1:200
Anti-CYP21A2	Sigma-Aldrich	HPA048979	1:200
Anti-AKR1B7 (M13)	Santa Cruz	sc-27763	1:200
Anti-3BHSD (P18)	Santa Cruz	sc-30820	1 :200
Anti-AR	Abcam	ab108341	1 :200
Anti-IBA1	Proteintech	10904-1-AP	1 :200
Anti-CD68	Proteintech	28058-1-AP	1:2000
Anti-DAB2 (E-11)	Santa Cruz	sc136964	1:50
Anti-BrdU (3D4)	BD Pharmingen	555627	1:100
Secondary antibodies	Source	Reference	Dilution
Donkey anti-rabbit Alexa Fluor 647	Invitrogen	A31573	1:400
Donkey anti-goat 555	Invitrogen	A21432	1:400
Donkey anti-mouse Alexa Fluor 555	Invitrogen	A31570	1:400
Biotinylated donkey anti-rabbit	Jackson Immunoresearch	711.065.152	1:400
Donkey anti-rabbit Alexa Fluor 555	Invitrogen	A31572	1:400
Donkey anti-mouse Alexa Fluor 647	Invitrogen	A31571	1:400